The molecular targets of ivermectin and lotilaner in the human louse Pediculus humanus humanus: New prospects for the treatment of pediculosis

Nicolas Lamassiaude, Berthine Toubate, Cédric Neveu, Pierre Charnet, Catherine Dupuy, Françoise Debierre-Grockiego, Isabelle Dimier-Poisson, Claude Charvet

HAL Id: hal-03148588

https://hal.science/hal-03148588

Submitted on 1 Jun 2021

PLOS PATHOGENS

The molecular targets of ivermectin and lotilaner in the human louse *Pediculus humanus humanus*: New prospects for the treatment of pediculosis

Nicolas Lamassiaude[1], Berthine Toubate[2], Cédric Neveu[1], Pierre Charnet[3], Catherine Dupuy[2], Françoise Debierre-Grockiego[2], Isabelle Dimier-Poisson[2]*, Claude L. Charvet[1]*

1 INRAE, Université de Tours, ISP, Nouzilly, France, **2** Université de Tours, INRAE, ISP, Tours, France, **3** Institut des Biomolécules Max Mousseron, UMR5247, CNRS, Université de Montpellier, Montpellier, France

* isabelle.poisson@univ-tours.fr (IDP); claude.charvet@inrae.fr (CLC)

Abstract

Control of infestation by cosmopolitan lice (*Pediculus humanus*) is increasingly difficult due to the transmission of parasites resistant to pediculicides. However, since the targets for pediculicides have no been identified in human lice so far, their mechanisms of action remain largely unknown. The macrocyclic lactone ivermectin is active against a broad range of insects including human lice. Isoxazolines are a new chemical class exhibiting a strong insecticidal potential. They preferentially act on the γ-aminobutyric acid (GABA) receptor made of the resistant to dieldrin (RDL) subunit and, to a lesser extent on glutamate-gated chloride channels (GluCls) in some species. Here, we addressed the pediculicidal potential of isoxazolines and deciphered the molecular targets of ivermectin and the ectoparasiticide lotilaner in the human body louse species *Pediculus humanus humanus*. Using toxicity bio-assays, we showed that fipronil, ivermectin and lotilaner are efficient pediculicides on adult lice. The RDL (Phh-RDL) and GluCl (Phh-GluCl) subunits were cloned and characterized by two-electrode voltage clamp electrophysiology in *Xenopus laevis* oocytes. Phh-RDL and Phh-GluCl formed functional homomeric receptors respectively gated by GABA and L-glutamate with EC_{50} values of 16.0 μM and 9.3 μM. Importantly, ivermectin displayed a super agonist action on Phh-GluCl, whereas Phh-RDL receptors were weakly affected. Reversally, lotilaner strongly inhibited the GABA-evoked currents in Phh-RDL with an IC_{50} value of 40.7 nM, whereas it had no effect on Phh-GluCl. We report here for the first time the insecticidal activity of isoxazolines on human ectoparasites and reveal the mode of action of ivermectin and lotilaner on GluCl and RDL channels from human lice. These results emphasize an expected extension of the use of the isoxazoline drug class as new pediculicidal agents to tackle resistant-louse infestations in humans.

Author summary

Human cosmopolitan lice are responsible for pediculosis, which represent a significant public health concern. Resistant lice against insecticides and lack of safety of the treatments for human and environment is a growing issue worldwide. Here we investigated the efficacy on lice of the classical macrocyclic lactone drug, ivermectin, and of the isoxazoline drug, lotilaner. This study was done to decipher their mode of action at the molecular and functional levels in order to propose new strategies to control lice infestation. Our bioassay results indicate that ivermectin and lotilaner were potent at killing human adult lice, with lotilaner showing a higher efficacy than ivermectin. Furthermore, we identified and pharmacologically characterized the first glutamate- and GABA-gated chloride channels ever described in human lice yet. Mechanistically, our molecular biology and electrophysiology findings demonstrate that ivermectin acted preferentially at glutamate channels, while lotilaner specifically targeted GABA channels. These results provide new insights in the understanding of the insecticide mode of action and highlight the potential of isoxazolines as a new alternative for the treatment of human lice.

Introduction

Lice are spread throughout the world in both low- and high-income countries, with heterogenous prevalence depending on the geographical area [1,2]. Pediculosis prevailing among school age children and homeless persons represents major economic, social but also public health concerns [3–8]. Human lice include the body louse *Pediculus humanus humanus* and the head louse *Pediculus humanus capitis* (order: *Phthiraptera*: Pediculidae). Both species are obligate blood feeding ectoparasites, living in clothes and in the scalp area, respectively [9]. Despite morphological, physiological and ecological differences, genetic studies showed that head and body lice have almost the same genomic and transcriptomic contents [9–11]. Furthermore, body lice are vectors of the pathogenic bacteria *Bartonella quintana*, *Borrelia recurrentis* and *Rickettsia prowazekii*, responsible for trench fever, louse-borne relapsing fever and epidemic typhus, respectively [4]. The control of lice infestation remains increasingly difficult due to the mode of transmission and the relative unreliable efficacy of the available treatments [12]. Even though silicon-based suffocating products are widely used nowadays, their efficacy largely depends on the respect of their application and is limited against the nits [13]. Chemical insecticides such as organochloride (lindane), organophosphates (malathion), carbamates (carbaryl) and pyrethroids (pyrethrins and synthetic permethrin), which are the first line treatments recommended by the Centers for Disease Control and Prevention and by the American Academy of Pediatrics, have been widely used to control lice [14,15]. They have been proposed to inhibit γ-aminobutyric acid (GABA)-gated chloride channels, acetylcholinesterase and voltage-gated sodium channels, respectively, leading to the paralysis of the parasite. However, louse resistance to these products has been widely reported [16–19] as well as neurotoxic effects in children and toxicity on the environment [20–25]. Because macrocyclic lactones (MLs) are broad-spectrum neuroactive insecticides, acaricides and nematicides used to treat and prevent endo- and ectoparasites of humans and animals [26], ivermectin (a derivate of the ML avermectins) has emerged as a promising pediculicide and quickly became the recommended molecule for the control of body lice [27–29]. In invertebrates, ivermectin binds to glutamate-gated chloride channels (GluCls) leading to a reduction in motor activity, paralysis and death. However, the molecular basis for the action of ivermectin in louse is unknown. Recently, treatment failures of ivermectin against lice were observed [30,31]. In that

respect, there is an urgent need to identify new druggable targets and develop new pediculicidal compounds.

Cys-loop ligand-gated ion channels (LGICs) are the major pharmacological targets of insecticides [32]. Among LGICs, the GluCls are found at inhibitory synapses of the nervous system exclusively in invertebrates [33], while GABA is the main inhibitory neurotransmitter in nerves and muscles in both vertebrates and invertebrates. GluCls and GABA receptors are constituted by the oligomerization of five identical or different subunits around a central pore [34]. In arthropods, the finding that the insecticidal activity of avermectins is mainly mediated by the GluCls was first achieved in the model insect *Drosophila melanogaster* [35]. For the GABA channels (GABACls), the screening for mutant flies that survive exposure to the insecticides dieldrin and fipronil, allowed the identification of the *resistant to dieldrin* gene or *rdl* [36]. When heterologously expressed in *Xenopus laevis* oocytes, the GluCl and RDL subunits formed functional homomeric glutamate-gated and GABA-gated chloride channels, respectively [35,37]. GluCl and RDL subunits were subsequently described in many other insect species although few of them were functionally assayed *in vitro*. Mutations in the GluCl subunit confers resistance to avermectins, whereas resistance to dieldrin, fipronil and picrotoxinin was shown to be associated to mutations in the RDL subunit using functional *in vitro* and *in vivo* experiments [32].

Interestingly, new synthetic molecules from the isoxazoline chemical class were recently proven to be effective ectoparasiticides against fleas and ticks [38]. The isoxazoline insecticides include fluralaner, afoxolaner, sarolaner and lotilaner [39–42]. They were shown to act as potent non-competitive antagonists of GABACls from *D. melanogaster* as well as the cat flea *Ctenocephalides felis* and the livestock tick *Rhipicephalus microplus* by molecular experiments and voltage-clamp electrophysiology. To a lesser extent, isoxazolines were also shown to act as antagonists of arthropod GluCls [39,43–45]. In addition, these compounds were efficient at blocking GABA-elicited currents from dieldrin- and fipronil-resistant channels. Recent studies on the actions of these compounds on cloned GABACls have accounted for their higher selectivity for insect over vertebrate receptors [42,43]. Compounds from the isoxazoline group are now considered as the next generation of broad-spectrum insecticides effective against veterinary, agricultural, sanitary and stored product pests from eleven arthropod orders [46]. However, the pediculicidal activity of isoxazolines, the identification of the target ion channels in lice and their potential use for human health have not been investigated so far.

The objectives of our study were to decipher the molecular targets of ivermectin and lotilaner in the human body louse species *Pediculus humanus humanus* (Phh). In the present paper, we describe in the human body louse: the *in vivo* pediculicidal activity, the target identification and *in vitro* mechanism of action of the phenylpyrazole insecticide, fipronil, the ML insecticide, ivermectin, and the last marketed isoxazoline, lotilaner. For this, we identified the human body louse orthologues of the GluCl and RDL subunit genes and subsequently achieved their respective functional characterizations in *Xenopus* oocytes using two-electrode voltage-clamp. We found that the Phh-GluCl and Phh-RDL subunits give rise to glutamate-gated and GABA-gated homomeric channels having distinct pharmacological properties. Hence, we provide mechanistic insights for a distinct mode of action of ivermectin and lotilaner. In the context of drug-resistance, this study highlights the pediculicidal potential of lotilaner and a possible extension of its use in new strategies to control human louse infestations.

Results

In vivo toxicity tests of ivermectin and lotilaner on lice and nits

In order to determine the efficacy of selected insecticides, we first performed insecticide exposure tests on laboratory-reared human adult body lice and nits (**Fig 1A**). Briefly, lice were
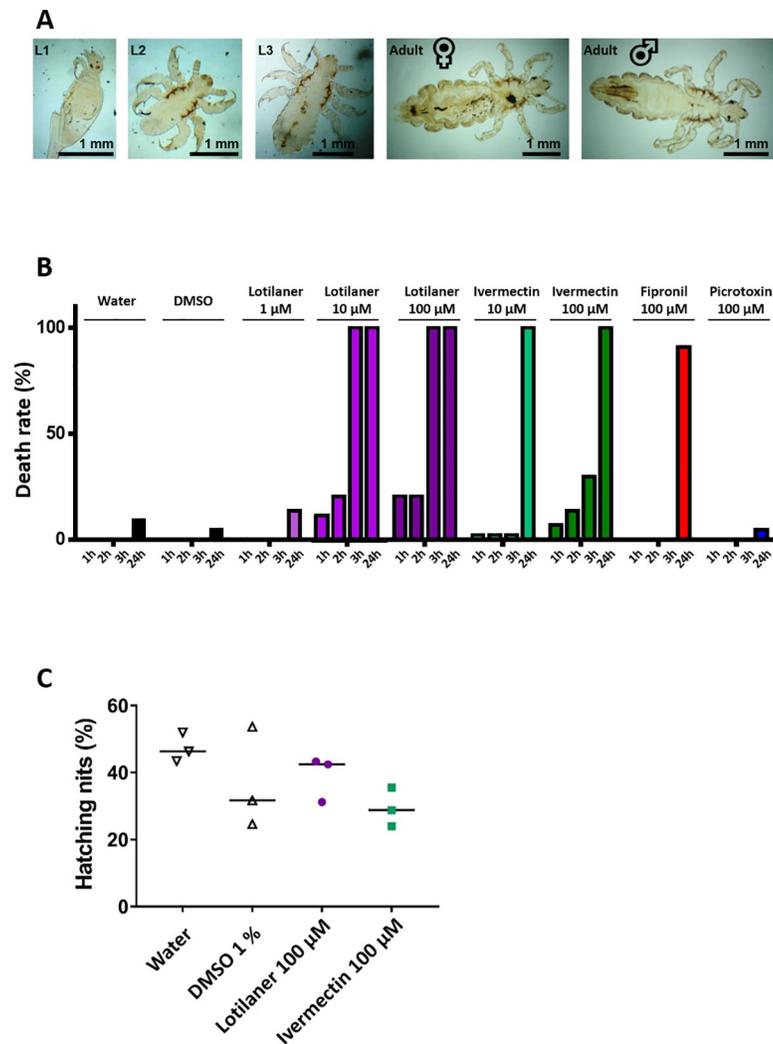
Fig 1. Toxicity tests on lice *in vivo*. A. Photographs of the human body lice from the laboratory-reared colony used in this study. Different life stages are represented from the left to the right: larvae in stage 1 during hatching (L1), larvae in stage 2 (L2), larvae in stage 3 (L3), female adult, male adult. **B.** Adult lice (n = 44 per condition) were treated with different concentrations of lotilaner, ivermectin, fipronil or picrotoxin and death or immobilization (knockdown) rate was determined throughout 24 hours. Water and 1% DMSO were used as negative controls. **C.** Nits were treated with 100 μM of lotilaner or ivermectin and hatching was determined between 6 and 9 days. Water and 1% DMSO were used as negative controls. The results are expressed as percentage of hatching from three independent experiments with n = 50 to 190 nits. The lines represent medians. The results are representative of three independent experiments.

https://doi.org/10.1371/journal.ppat.1008863.g001

incubated with ivermectin, fipronil, picrotoxin and lotilaner at different concentrations. The effects of the compounds on louse survival and immobilization (**S1 Table** for knockdown groups) were subsequently analyzed at four timepoints (1, 2, 3, and 24 hours). After 24h, there was 4.5% mortality in the groups of lice treated with 1% DMSO that was used to dissolve the different compounds (**Fig 1B** and **S2 Table**). Similarly, 100 μM picrotoxin was not efficient to kill the lice after 24h whereas 91% of the lice were killed or immobilized with exposure to 100 μM fipronil at the same time. In our experiments, fipronil was used as a positive control and this result corroborated previous bioassays in the literature [47]. As expected, ivermectin was more efficient than fipronil, since the death rate reached 30%, 3h after application of

100 μM, and 100% after 24h application of both 10 and 100 μM (**Fig 1B**). These findings confirmed the insecticide susceptible status of the laboratory-reared colony used here. Strikingly, after application of 100 μM lotilaner, the number of living lice declined rapidly. Not only the application of 1 μM lotilaner killed 14% of lice at 24 h but 10 and 100 μM lotilaner led to the death of all lice 3h after exposition (**Fig 1B**). Interestingly, when compared with other drugs, 10 μM lotilaner was more efficient than 10 μM ivermectin and 100 μM fipronil. Next, we analyzed the effect of 100 μM ivermectin or lotilaner on the nit hatching between six and nine days after drug application. The rate of nits hatched did not differ between the ivermectin- and the lotilaner-treated nits and the negative controls (water and 1% DMSO) thus revealing the absence of efficacy of the two products on the nits (**Fig 1C**). Altogether, these results confirm that fipronil and ivermectin are efficient at killing human adult body lice and provide the first *in vivo* evidence of a pediculicidal activity for lotilaner. These data prompted us to investigate the targets of ivermectin and lotilaner at the molecular level.

GluCl and RDL subunits are conserved in *P. humanus humanus*

Macrocyclic lactones and isoxazolines were previously shown to act both on arthropod glutamate- and GABA-gated channels. Therefore, we decided to identify and clone the respective *P. humanus humanus* GluCl and RDL subunits through a candidate gene approach. Searches for homologues of *A. mellifera* and *D. melanogaster* GluCl and RDL receptor subunits in *P. humanus* genomic/transcriptomic databanks, allowed the identification of two independent coding sequences for *Phh-glucl* and for *Phh-rdl* for which the respective complete coding sequences were obtained by RACE PCR experiments. All louse GluCl and RDL displayed the characteristic features of cys-loop LGIC subunits, including a signal peptide, an extracellular N-terminal domain containing the ligand binding sites, a disulfide bond formed by two cysteines that are 13 amino acid residues apart (cys-loop domain), four transmembrane domains (TM1-TM4) and a large intracellular loop between TM3 and TM4 that is highly variable (**Fig 2A**). Of importance is the sequence analysis of the pore selectivity filter located in the TM2 supporting the prediction with the signature of a chloride channel. Indeed, Phh-GluCl and Phh-RDL contain the PAR motif centered at the 0' position in the TM2 and conserved in other species (universal LGIC TM2 numbering system). A proline at position -2', followed by a small amino acid at position -1' like an alanine, an arginine at the 0' residue and a threonine at position 13' are the hallmarks of chloride–permeable LGICs [48].

The full-length coding sequences for the GluCl subunits included ORFs of 1353 and 1350 bp encoding proteins of 450 and 449 amino acids that were named Phh-GluCl-1 (MT321070) and Phh-GluCl-2 (MT321071), respectively. The alignement of *Phh-GluCl-1* and *Phh-GluCl-2* deduced amino-acid sequences is provided in **Fig 2A**. The two sequences are highly conserved with 97% identity and 98% similarity and only differ by eleven amino acid substitutions and an alanine insertion in the N-terminal part at position 59 in Phh-GluCl-1. (**Figs 2A** and S1). Noteworthy, all the amino acids involved in the glutamate binding were conserved.

For RDL subunits, both full-length coding sequences are 1467 nucleotide long encoding 489 amino acids. Phh-RDL-1 (MT321072) and Phh-RDL-2 (MT321073) share 96% identity and 98% similarity, only differing by 20 amino acid substitutions including 17 amino acid changes located in the extracellular N-terminal region between the signal peptide and the TM1 (**Figs 2A** and S2). Notably, none of the residues involved in the binding of GABA were subjected to substitutions. The conserved amino acids in TM1, TM2 and TM3, known to be related to the effect of fluralaner on *Musca domestica* RDL and GluCl [49,50], are indicated with purple asterisks in **Fig 2A**. These included Q267, I270, L274, A295, D325, G329, F332, V333 for Phh-RDL and Q241, I244, M248, S279, D309, G313, L316, T317 for Phh-GluCl.
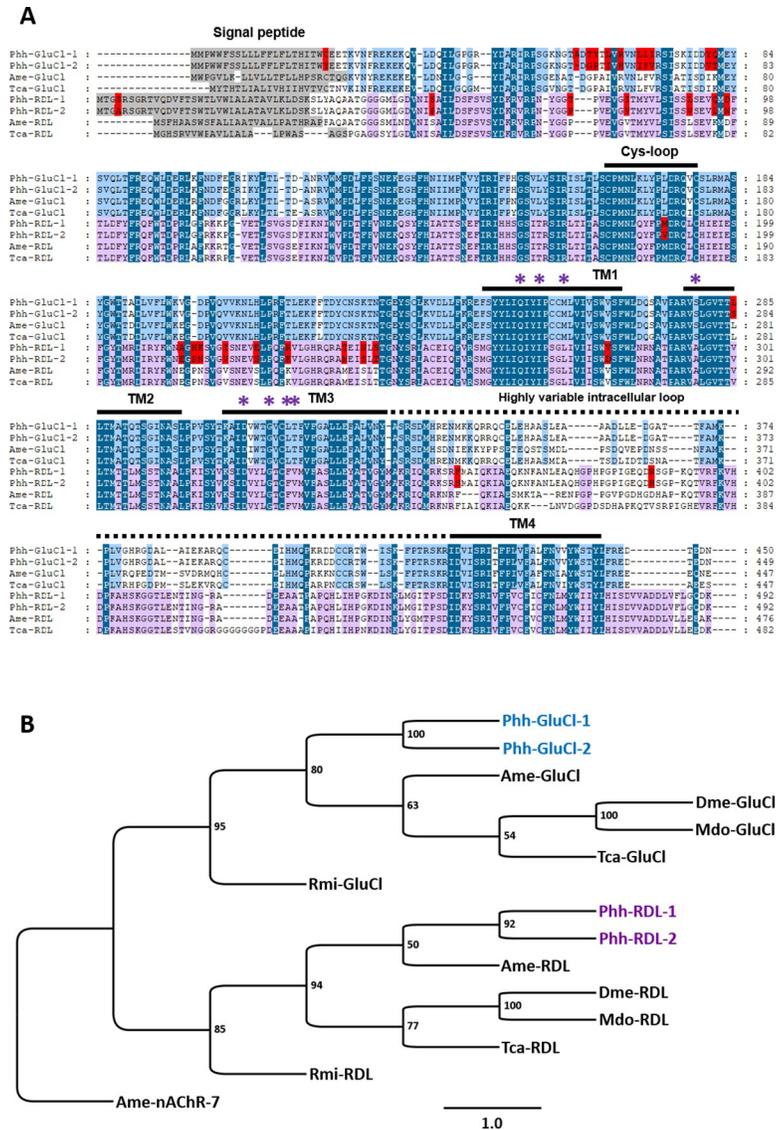
Fig 2. Comparison of GluCl and RDL subunits. A. Amino acid alignments of GluCl and RDL subunit sequences of *Pediculus humanus humanus*, *Apis mellifera* and *Tribolium castaneum*. Predicted signal peptides in the N-terminal region are highlighted in grey. Amino acid differences between Phh-GluCl-1 and Phh-GluCl-2 or between Phh-RDL-1 and Phh-RDL-2 sequences of *P. humanus humanus* are highlighted in red. Cys-loop domain, predicted transmembrane domains TM1 to TM4 and the highly variable intracellular loop are indicated by the bars. Amino acids conserved between all the sequences are highlighted in dark blue. Amino acids conserved between GluCl sequences are highlighted in light blue. Amino acids conserved between RDL sequences are highlighted in pink. Purple asterisks represent amino acids docking for fluralaner based on previous studies [43, 79]. **B.** Distance tree (BioNJ, Poisson) of GluCl and RDL protein sequences from insects and acarians. The three letter prefixes in gene names Phh, Ame, Tca, Dme, Mdo and Rmi refer to the species *Pediculus humanus humanus*, *Apis mellifera*, *Tribolium castaneum*, *Drosophila melanogaster*, *Musca domestica* and *Rhipicephalus microplus*, respectively. Branch lengths are proportional to the number of substitutions per site. Scale bar represents the number of substitutions per site. The bootstrap values are indicated next to each branch. Accession numbers for sequences used in the phylogenetic analysis are provided in the Methods section. Sequences of *P. humanus humanus* are highlighted in blue for GluCls and purple for RDLs. The *A. mellifera* alpha7 nAChR subunit sequence was used as an outgroup.

A distance tree analysis of *P. humanus humanus* GluCl and RDL sequences including *D. melanogaster*, the honey bee *Apis mellifera*, the house fly *Musca domestica*, *R. microplus* and the red flour beetle *Tribolium castaneum* confirmed the orthologous relationships of the louse

subunit sequences with their respective counterparts (**Fig 2B**). GluCl amino acid sequences revealed that Phh-GluCls were found to be highly conserved, sharing 78%, 84%, 81% and 70% identities with the respective orthologues from *A. mellifera*, *T. castaneum*, *D. melanogaster* and *R. microplus*. Phh-RDL-1 and 2 shared 84%, 81%, 67% and 54% identities with their orthologues from *A. mellifera*, *T. castaneum*, *D. melanogaster* and *R. microplus*, respectively. These observations are in accordance with the relative position of Phthiraptera and Hymenoptera insect subfamilies and Acarids [49] and were further confirmed by supplementary analysis including other members from the GABA and GluCl groups from additional arthropod species (**S1** and **S2** **Figs**). In the phylogeny of GABA subunits, Phh-RDL-1/-2 were found to clearly cluster distinctly from the LCCH3, GRD and 8916 subunits, showing that each species has inherited an ancestral gene. Altogether, the phylogenetic observations support that we cloned the *P. humanus humanus* GluCl and RDL subunit orthologues allowing their subsequent assessment at the functional level.

P. humanus humanus GluCl and RDL subunits form functional homomeric channels in *Xenopus* oocytes

In previous studies, arthropod GluCl and RDL subunits were shown to reconstitute functional channels when expressed in *Xenopus* oocytes [32]. Hence, we hypothesized that the ortholog subunits from *P. humanus humanus* could form functional receptors. Following the cloning of two full-length coding sequences for Phh-GluCl and Phh-RDL subunits, their respective cRNAs were microinjected in *X. laevis* oocytes. To investigate the receptor functionality, responses to agonists were assessed by two-electrode voltage-clamp (TEVC) electrophysiology. In sharp contrast with Phh-GluCl-1 and Phh-RDL-1 subunits (**Fig 3**), injections of *Phh-GluCl-2* (n = 11) and *Phh-RDL-2* (n = 12) cRNAs never led to recordings of glutamate- and GABA-evoked currents, respectively, indicating that these subunits did not form functional receptors (**S3 Fig**). Thus, Phh-GluCl-1 and Phh-RDL-1 will be henceforth refered to as Phh-GluCl and Phh-RDL in the article. When glutamate was perfused in the recording chamber, we could record fast inward currents in the μA range in oocytes injected with *Phh-GluCl* (**Fig 3A**). As expected, this receptor desensitized extremely rapidly upon prolonged glutamate exposure. Then, we obtained the concentration-response curve by challenging the oocytes with glutamate concentrations ranging from 1 to 1000 μM. With current amplitudes normalized to the maximal response to 1000 μM, we found that the glutamate EC_{50} value of Phh-GluCl was 9.3 +/- 1.3 μM with a Hill coefficient of 1.9 +/- 0.5 (n = 5) suggesting the presence of more than one glutamate binding site (**Fig 3A and 3B**). When *Phh-RDL* cRNAs were injected in oocytes, the application of 100 μM GABA resulted in robust currents with maximum amplitudes in the μA range (**Fig 3D**). The GABA concentration-response curve was characterized by an EC_{50} of 16.0 +/- 0.4 μM (n = 6) with a Hill coefficient of 2.3 +/- 0.1 (n = 6) suggesting the binding of more than two GABA molecules (**Fig 3E**). As previously shown in the literature, RDL and GluCls are permeable to chloride anions [35,37,50–53]. Here, the TM2 amino acid sequences of Phh-RDL and Phh-GluCl are respectively 100% identical with RDL and GluCls from other insect species such as *A. mellifera*, *D. melanogaster*, *T. castaneum* (**Fig 2A**), suggesting they are anionic receptors. In order to investigate the ion selectivity, we applied voltage-ramps to oocytes expressing Phh-GluCl or Phh-RDL and measured the reversal potentials for the respective glutamate- and GABA-sensitive currents in recording solution with varying concentrations of either chloride or sodium. Then, the reversal potentials were plotted against the chloride or sodium concentration (**Fig 3C and 3F**). In the standard recording solution containing 100 mM NaCl, glutamate-induced currents reversed at -23.39 +/- 1.26 (n = 12) (**Fig 3C**). When the extracellular chloride concentration decreased from 104.5 to 4 mM
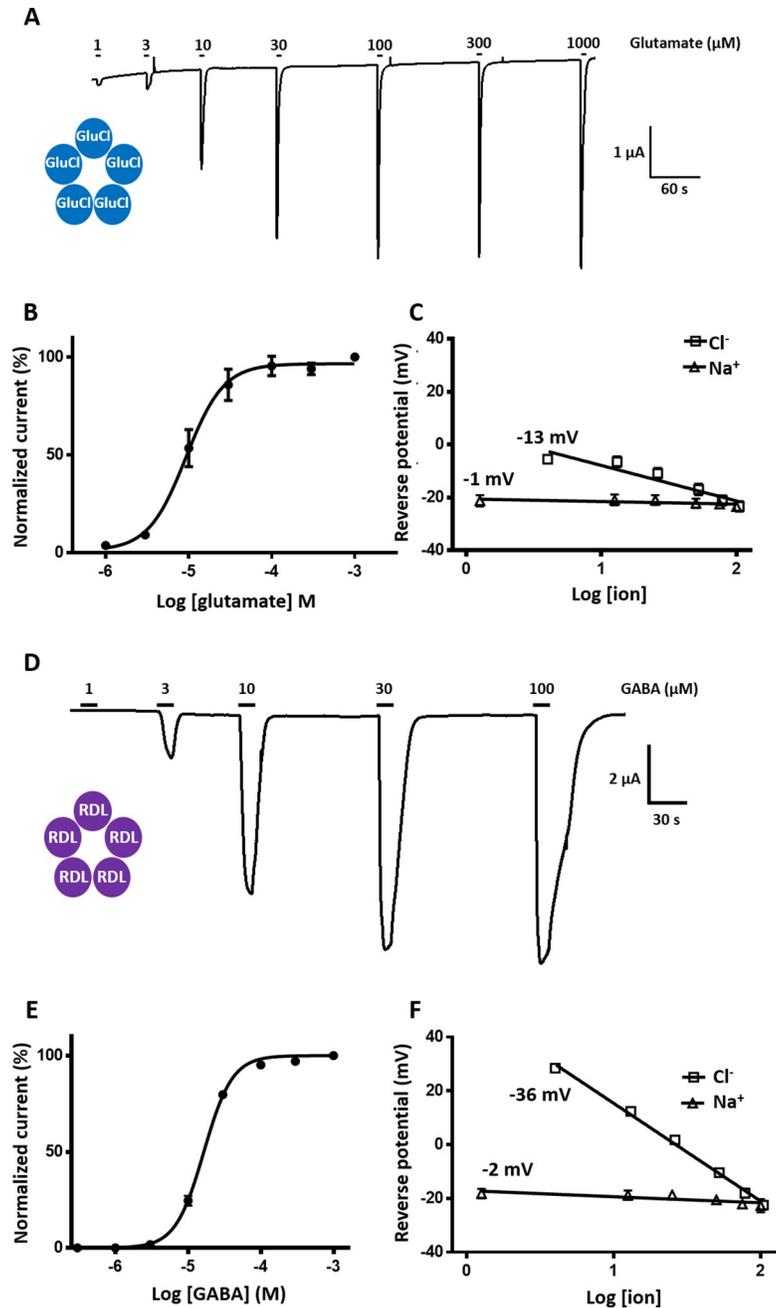
Fig 3. Functional expression of Phh-GluCl and Phh-RDL channels in *X. laevis* oocytes. A. Current traces recorded on oocytes injected with Phh-GluCl cRNA in response to the application of 1 to 1000 μM of glutamate. Oocytes were clamped at -80 mV. Application times are indicated by the bar. **B.** Glutamate concentration-response curve for Phh-GluCl (mean +/- SEM, n = 5 oocytes). Data were normalized to the maximal effect of glutamate. **C.** Reverse potential-ion concentration relationships of oocytes expressing Phh-GluCl obtained from voltage-ramps in presence of glutamate and using increasing concentrations of either Cl⁻ or Na⁺ to analyze the selectivity of this channel. **D.** Current traces recorded on oocytes injected with Phh-RDL cRNA in response to the application of 1 to 100 μM of GABA. Oocytes were clamped at -60 mV. Application times are indicated by the bars. **E.** GABA concentration response curve for Phh-RDL (mean +/- SEM, n = 6 oocytes). Data were normalized to the maximal effect of GABA. **F.** Reverse potential-ion concentration relationships of oocytes expressing Phh-RDL obtained from voltage-ramps in presence of GABA and using increasing concentrations of either Cl⁻ or Na⁺ to analyze the selectivity of this channel.

(replacement of chloride by sodium acetate), Phh-GluCl exhibited a 13.4 +/- 2.3 mV shift upon a 10-fold change in the chloride concentration (n = 7). In contrast, decreasing the extracellular sodium concentration from 100 to 0 mM (replaced by tetraethylammonium chloride) did not significantly shift the reversal potential (1.0 +/- 0.5 mV shift per decade, n = 47). Similarly, Phh-RDL was highly sensitive to the extracellular chloride concentration (36.4 +/- 1.2 mV shift upon a 10-fold change in the chloride concentration, n = 4), whereas it was almost insensitive to variations of the extracellular sodium concentration (2.3 +/- 0.8 mV shift per decade, n = 4) (**Fig 3F**). These results indicate that both Phh-GluCl and Phh-RDL form chloride permeable GABA-gated channels that do not permeate sodium ions, consistently with the pore selectivity filter sequence (**Fig 2A**) and channels from other species [53,54]. In summary, these findings demonstrate that two novel functional homomeric receptors from the human body louse, Phh-GluCl and Phh-RDL, with respectively high affinity to glutamate or GABA, were reconstituted in *Xenopus* oocytes.

Differential effects of ivermectin and lotilaner on *P. humanus humanus* GluCl and RDL channels

Arthropod GluCl and RDL channels are well-known targets for insecticides [32]. In order to investigate their respective insecticides sensitivities, Phh-GluCl and Phh-RDL were challenged with ivermectin, lotilaner, fipronil and picrotoxin. Recordings from oocytes expressing Phh-GluCl revealed that ivermectin is a potent agonist of this receptor. A slow activation of the receptor was observed with application of ivermectin as low as 10 nM and large μA currents were recorded in response to 1 μM ivermectin with an average of 86.5 +/- 8.2% (n = 6) of the 1 mM glutamate-elicited current (**Fig 4A**). The dose-response curve (**Fig 4B**) revealed an ivermectin EC_{50} of 78.52 +/- 30.22 nM (n = 3–9). As expected, the effect of ivermectin was not reversible. When applied on Phh-GluCl expressing oocytes, 1 to 30 μM lotilaner did not elicit any current and mediated no significant inhibitory effect on glutamate-evoked currents (p > 0.057) (**Fig 4C and 4D**). We subsequently tested the activity of selected insecticides on the Phh-RDL channel. As anticipated from the literature, lotilaner, picrotoxin and fipronil had no agonist effect (**Fig 5**). Interestingly, applications of 0.3 to 30 μM ivermectin during 90 seconds on Phh-RDL elicited slow and sustained currents which were not reversible (**S4A Fig**). The maximum effect corresponding to 7.9 +/- 1.3% (n = 6) of the 1 mM glutamate response was obtained with 1 μM ivermectin (**S4B Fig**). Then, we investigated the potential antagonistic effects of the selected insecticides on GABA recording traces. **Fig 5A–5D** illustrates results from application of 100 μM GABA before, during and after the sequential addition of increasing concentrations of insecticide. GABA-elicited currents were completely inhibited with 3 μM fipronil, ivermectin and lotilaner. On the other hand, picrotoxin had a weaker effect on Phh-RDL since the full inhibition of the GABA elicited current was observed with 30 μM. In accordance with the litterature [55], ivermectin acted as an inhibitor of Phh-RDL. More importantly, GABA responses were totally and irreversibly blocked with lotilaner as low as 0.3 μM suggesting that Phh-RDL is more sensitive to lotilaner than to the other insecticides fipronil, picrotoxin and ivermectin. To characterize this effect, concentration-inhibition response relationships were performed for the four drugs (**Fig 5E**). Picrotoxin, ivermectin and fipronil antagonized Phh-RDL in a concentration-dependent manner with IC_{50} values of 1.16 +/- 0.23 μM (n = 6), 342.5 +/- 14.0 nM (n = 6) and 137.5 +/- 35.1 nM (n = 6), respectively. Lotilaner resulted in the most potent dose-dependent inhibition of the GABA-mediated currents with an IC_{50} value of 40.7 +/- 6.8 nM (n = 6) (**Fig 5E**). Rank order potency series for each of the Phh-RDL antagonists tested was as follows: lotilaner > fipronil > ivermectin > picrotoxin. In order to determine the type of inhibition caused by lotilaner and ivermectin on Phh-RDL,
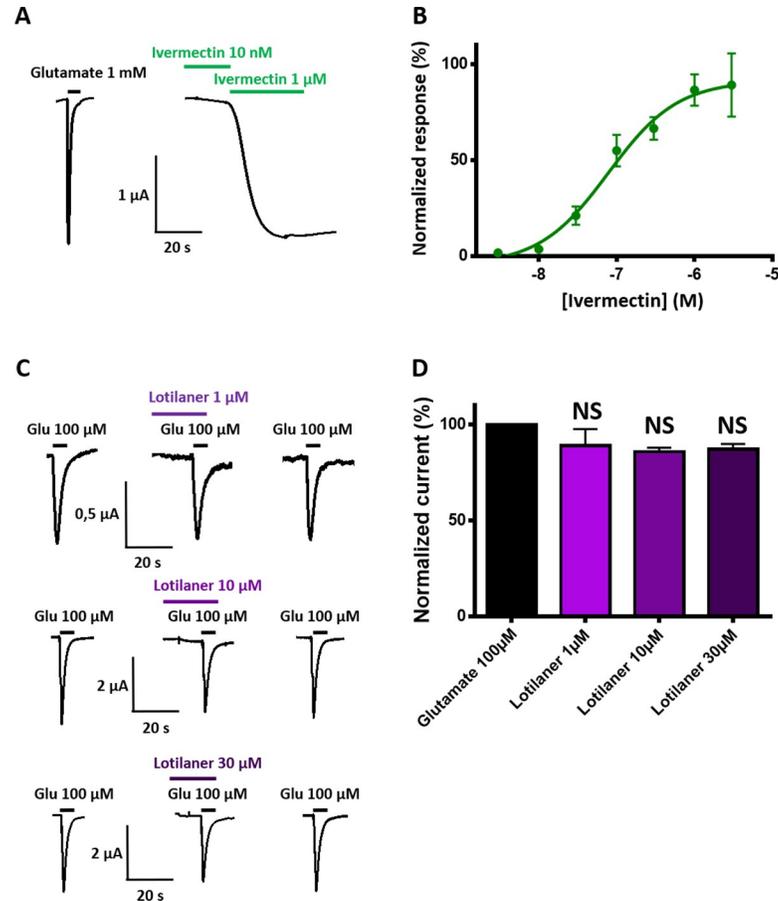
Fig 4. Effects of ivermectin and lotilaner on Phh-GluCl receptor in *X. laevis* oocytes. A. Representative current traces from a single oocyte expressing Phh-GluCl challenged with 1 mM glutamate and 10 nM ivermectin followed by 1 μM ivermectin. The bars indicate the time period of agonist application. **B.** Ivermectin concentration-response curve for Phh-GluCl (mean +/- SEM, n = 5 oocytes). Data were normalized to the current amplitude of a first application of 100 μM of glutamate. **C.** Representative current traces from oocytes perfused with 100 μM glutamate (Glu) alone (left), with 1–30 μM lotilaner prior to co-application with 100 μM Glu (middle) and after wash out (right). **D.** Bar chart (mean + SEM, n = 5) of the response elicited by co-application of 100 μM glutamate with 1–30 μM lotilaner normalized to and compared with the response to 100 μM glutamate alone (One-way ANOVA with Tukey's Multiple Comparisons Test, NS: Not Significative).

https://doi.org/10.1371/journal.ppat.1008863.g004

we performed a competitive experiment (**Fig 6**). Briefly, a fixed concentration of lotilaner (1 nM and 10 nM) or ivermectin (100 nM and 1 μM) was continuously applied on oocytes while performing a GABA dose-response. The EC_{50} values and maximum current amplitudes were 16.0 +/- 0.4 μM and 97.95 +/- 0.69% (n = 6) for GABA alone, 14.3 +/- 1.9 μM and 69.16 +/- 2.54% (n = 5) in the presence of 1 nM lotilaner and 11.5 +/- 4.0 μM and 48.56 +/- 4.90 (n = 6) in the presence of 10 nM lotilaner (**Fig 6A**). The presence of lotilaner did not significantly change the GABA EC_{50} (p > 0.49 and p > 0.32 for 1 nM and 10 nM, respectively) but reduced significantly the maximum current amplitudes obtained with a saturating GABA concentration (p < 0.0001), which is a characteristic feature of a non-competitive antagonism. The competition experiment with ivermectin showed the remarkable ivermectin mode of action on Phh-RDL. Indeed, coapplication of low ivermectin concentration (100 nM) and low GABA concentration (3 μM) increased the current amplitude compared to the application of GABA alone highlighting the potentiation effect of ivermectin (**Fig 6B**). A higher concentration of ivermectin (1 μM) had a dual mode of action with a weak current activation (**S4 Fig**) and an
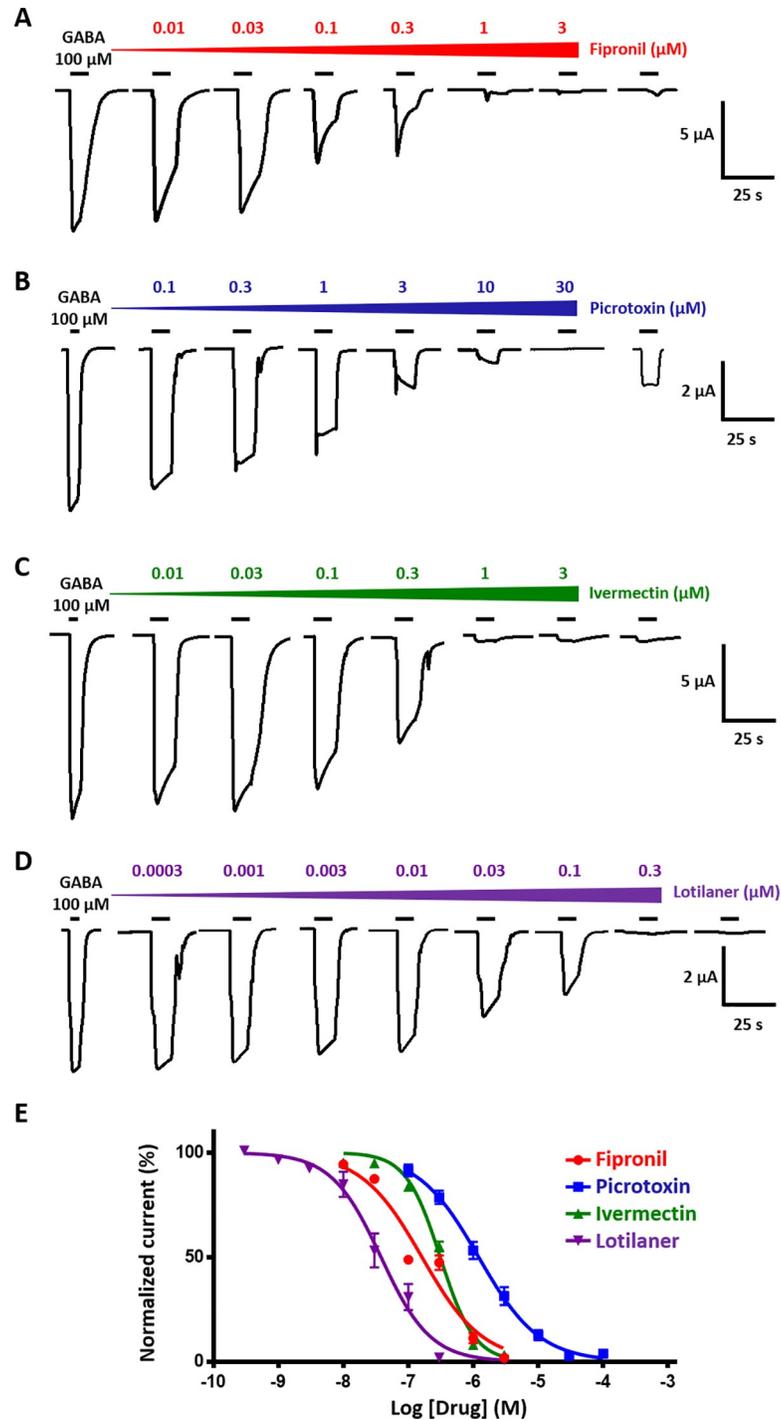
Fig 5. Antagonistic effects of fipronil, picrotoxin, ivermectin and lotilaner on GABA-elicited currents in *X. laevis* oocytes expressing Phh-RDL receptor. A-D. Representative current traces evoked by 100 μM GABA alone or with co-application of increasing concentrations of fipronil, picrotoxin, ivermectin and lotilaner. After antagonist application, a last 100 μM GABA application was performed to assess their reversible potential. Application times are indicated by the bars. **E.** Concentration-inhibition curves for Phh-RDL for fipronil (red circles, n = 6–7), picrotoxin (blue squares, n = 6), ivermectin (green triangles, n = 6) and lotilaner (purple triangles, n = 6). Data are all normalized to the response to 100 μM GABA (mean +/- SEM).
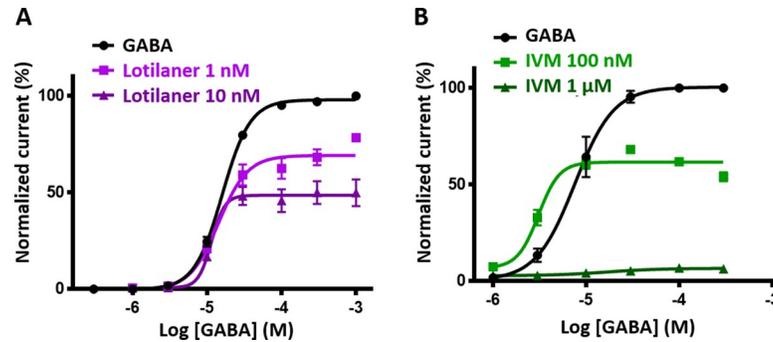
Fig 6. Competitive assay for lotilaner and ivermectin on Phh-RDL. A. Lotilaner is a non-competitive antagonist of Phh-RDL. GABA concentration-response curves were performed with GABA alone (black circles) or with lotilaner at 1 nM (purple squares) and 10 nM (purple triangles). Data were normalized to a first application of 100 μM GABA (mean +/- SEM, n = 5–6). **B**. Dual action of ivermectin on Phh-RDL. GABA concentration response were performed with GABA alone (black circles) or with ivermectin at 100 nM (green squares) and 1 μM (green triangles). Data were normalized to a first application of 100 μM GABA (mean +/- SEM, n = 5–6).

https://doi.org/10.1371/journal.ppat.1008863.g006

inhibition of the GABA-elicited current indicating both an agonistic and antagonistic effect of ivermectin (**Fig 6B**). Altogether, these results demonstrate that *P. humanus humanus* GluCl and RDL characterized in *Xenopus* oocytes display original pharmacologies regarding insecticides. Ivermectin acted as a strong agonist of Phh-GluCl while showing a double action on Phh-RDL with agonist or antagonist effects depending on the concentration. Finally, the antiticks and fleas lotilaner had no effect on Phh-GluCl, while it was a potent and selective non-competitive antagonist of RDL of human lice.

Discussion

First functional characterization of LGICs from human lice

In the present study, we report the first functional expression and pharmacological characterization of any human louse LGICs. Indeed, despite the social and public health impacts of human lice and the growing issue of resistance to pediculicides and since the complete sequencing of the body louse genomes, there was to our knowledge no functional characterization of any LGICs from lice so far [10,29]. Because glutamate and GABA are important neurotransmitters in the insect central nervous system and their receptors are targets for insecticides, we focused our attention on glutamate- and GABA-sensitive receptors. GluCl and RDL channel subtypes of LGICs have been extensively characterized in many arthropod species starting with the model fruit fly *D. melanogaster* and ranging from agricultural and sanitary pests to animal ectoparasites and disease vectors, but also beneficial insects like the honey bee [32,33]. Here, we show that *P. humanus humanus* GluCl and RDL subunits gave rise to homomeric channels when functionally expressed in *Xenopus* oocytes. This experimental expression system provided a unique means to assess the pharmacological and biophysical properties of these receptors. Even though two putative genes encoding respectively a GluCl and a GABA receptor have been identified in the genomic database, the molecular cloning of complete cDNAs revealed at least two potential full-length transcripts for both candidates (i.e. Phh-GluCl-1, Phh-GluCl-2 and Phh-RDL-1, Phh-RDL-2). These transcripts could either be alternative spliced isoforms or result from RNA A-to-I editing, a mechanism of RNA edition described in lice [56]. In insects, alternative splicing and RNA A-to-I editing are known to increase diversity of LGICs subunits [57–60]. Undoubtedly, further molecular investigations at the DNA level would be required to confirm this hypothesis. Here, we report that both Phh-

GluCl-1 and Phh-RDL-1 can be robustly expressed in *Xenopus* oocytes, whereas neither Phh-GluCl-2 nor Phh-RDL-2 subunits formed functional receptors in our conditions. Interestingly, Phh-GluCl had one of the highest affinity for glutamate compared to other GluCls of arthropod species (*Drosophila*, *Musca*, *Caligus*, *Ixodes*, *Plutella*, *Tetranychus*, *Laodelphax*, and *Anopheles*), the reported EC_{50} of which varied between 6.89 μM in *Caligus rogercresseyi* and 3.019 mM in *Tetranychus cinnabarinus* [35,43,50–52,61–65]. Likewise, Phh-RDL had one of the lowest EC_{50} for GABA among described insect RDL receptors showing EC_{50} varying between 5.43 +/- 0.02 μM in the brown planthopper *Nilaparvata lugens* [66] and 445 +/- 47 μM in the carmine spider mite *Tetranychus cinnabarinus* [64] with the exception of the RDL-2 subunit (2.4 +/- 0.3 μM) from the honey bee parasite mite *Varroa destructor* [53]. Similarly, spliced variant transcripts of GluCl and RDL subunits were found to give rise to functional channels in several insect species, thus increasing their receptor diversity [33,59,60,63,65,67–69]. Here, we identified and characterized the first GluCl and GABACl receptors of human lice. This study opens the way for the characterization of other receptor subtypes, which can also be relevant targets.

New insights into the mode of action of ivermectin on lice

Despite the massive use of pediculicidal compounds during the past decades, there was to our knowledge no functional characterization of their molecular targets in lice. Macrocyclic lactones are widely used in both veterinary and human medicine, with ivermectin being typically the recommended molecule for the control of body lice [27–29]. This broad-spectrum drug is highly efficient against a wide range of pathogens including endo- and ectoparasites such as nematodes, acarians and insects [26]. In comparison with other pediculicides, ivermectin presents some major advantages. First, it has long been recognized that it is a safe pharmaceutical in human health due to low level of toxicity for mammalians, in sharp contrast with classical pediculicides [70]. Indeed, former drugs such as fipronil, lindane or malathion are now forbidden for human use in several countries because of their toxicity and environmental impact [20–25]. Second, ivermectin is currently the only molecule used as an oral treatment against lice. For head lice, oral route avoids suboptimal shampoo application, thus reducing the emergence and transmission of resistant lice [28,71–73]. For body lice, oral dosing is of particular interest to treat people having a limited access to basic hygiene services. However, despite these remarkable advantages, ivermectin's efficacy is currently compromised by the emergence of resistant lice [30,31].

Here, our bioassay confirmed the pediculicidal activity of ivermectin on human body lice. Furthemore, we addressed for the first time the mode of action of ivermectin at the molecular level on louse glutamate- and GABA-gated receptors. We showed that ivermectin preferentially activated Phh-GluCl channel, and Phh-RDL in a much lower extent. In addition, ivermectin blocked the RDL receptor with an IC_{50} 4-fold higher than the ivermectin EC_{50} for Phh-GluCl. Hence, these findings suggest that Phh-GluCl is the preferential target of ivermectin. Interestingly, functional silencing using RNAi has already been shown to be an efficient and promising approach to investigate the role of detoxification genes in ivermectin tolerance of human body lice [74]. In order to confirm that GluCl is the main target of ivermectin in lice, it would be interesting to explore *in vivo* the phenotype of *Phh-GluCl* siRNA silenced lice as previously demonstrated for abamectin in *T. cinnabarinus* and in the crop whitefly pest *Bemisia tabaci* [64,75]. Finally, following the recent observation of GluCl single-nucleotide-polymorphisms (SNPs) in phenotypically ivermectin-resistant head lice [30], our results provide a unique means to explore the molecular mechanisms underlying louse resistance to ivermectin. In a further step, such electrophysiology studies in *Xenopus* oocytes will enable to determine the functional relevance of GluCl SNPs detected in ivermectin-resistant lice [51,55,62,76,77].

Although the putative role of those SNPs are to be determined, we can reasonably assume that mutated subunits can lead to GluCl altered functionality, probably resulting in ivermectin resistance. Additionaly, screening on ivermectin-resistant GluCls recombinantly expressed will provide a powerful tool to optimize the design of new pediculicidal compounds. Further investigations are required to understand the mechanisms of ivermectin resistance and to define new control strategies to avoid emergence of resistance as well as to preserve this molecule efficacy.

On the mode of action of isoxazolines in arthropods

With the recent introduction of new generation of compounds in the isoxazoline class (e.g. lotilaner), the development of detailed understanding of the actions of isoxazolines is essential. Arthropod RDL channels are major targets for several insecticidal classes including dieldrin itself and fipronil [32] and they were recently shown to be the primary target for isoxazolines [39–43]. Therefore, we hypothesized that they could act on RDL from *Pediculus humanus humanus*. In addition to the pharmacological characterization of Phh-RDL and Phh-GluCl, our results show that the inhibitory effects of lotilaner depend on the receptor subtype. Indeed, lotilaner efficiently and selectively blocked the GABA response on Phh-RDL, whereas Phh-GluCl was not affected, even with the use of a concentration of 30 μM representing 737-fold the lotilaner IC_{50} for Phh-RDL. In order to confirm these findings, it will be interesting to silence the *rdl* gene using RNAi in human body lice [64]. Our results clearly demonstrated the selective antagonistic action of lotilaner on RDL over GluCl channels contrary to fluralaner, which was reported to inhibit both RDL and GluCls from *M. domestica* and *R. microplus* [39,43,78,79]. Whether these differences might be due to the compounds themselves or the pharmacological properties of receptors from different species remain to be investigated. Although some studies recently indicated that four amino acids in the transmembrane subunit interface were closely related to the antagonism of *M. domestica* RDL by fluralaner [79], the mechanism of action of lotilaner on RDL receptors at the molecular level remains to be deciphered. Likewise, further efforts are needed to better understand the molecular basis of the insect selectivity of isoxazolines over vertebrate channels. Contrary to homomeric arthropod RDL channels, the vertebrate GABA are heteromeric channels made of different subunits. Recent studies indicated that fluralaner and lotilaner were highly selective of arthropod RDL channels, while poorly efficient on rat brain membranes ($IC_{50} > 10$ μM), rat GABA channels ($IC_{50} > 30$ μM) and canine GABA channels ($IC_{50} > 10$ μM), thus evidencing for low mammalian toxicity [39,42,43]. Resistance to isoxazolines has not been reported so far and dieldrin resistance is likely not to confer cross-resistance to fluralaner [43]. Furthermore, the antagonistic effect of fluralaner and lotilaner on RDL receptors from *M. domestica* and *D. melanogaster* was not impaired by known mutations confering fipronil and dieldrin resistance [42,43]. Likewise, the distinct mechanisms of action for ivermectin and lotilaner seem to indicate that resistance to ivermectin will not extend to the isoxazolines. Identification of homologous genes encoding RDL subunits and investigation of new expressed recombinant RDL from many other arthropod species including important insect pest species, acari and crustaceans will enhance our understanding of the action of isoxazolines. The potency and selectivity of isoxazolines indicate an important future for this class of compounds.

From dog to human: Isoxazoline insecticides as promising pediculicidal candidates

The isoxazoline class is a new generation of insecticidal compounds recently introduced for insect chemical control including ectoparasites such as acari and fleas [44,45]. Since the

discovery of isoxazolines, their insecticidal spectrum has become broader to agricultural, sanitary and animal insect pests belonging to eleven orders missing out the order of *Phthiraptera* [39–43,45,46]. In the present study, we hypothesized that the isoxazolines could represent attractive candidate drugs to extend the pharmacopeia for louse control. Among the different compounds from the isoxazoline family, we selected the insecticide lotilaner as a proof-of-concept model for the isoxazoline effectiveness as pediculicidal for human use. Isoxazolines are licensed for protection of companion animals against fleas and ticks and therefore present a reduced toxicity to mammals. In addition, isoxazolines have a long-lasting effect after a single oral administration [42,80]. In dogs, lotiIaner remains active against ticks and fleas during one month with an efficacy ranging from 98 to 100% [81,82]. Here, we assessed the pediculicidal potential of lotilaner against different stages of body lice. Strikingly, our bioassays on human body lice demonstrated that the adulticide effect of lotilaner was higher than that of ivermectin and fipronil. Whereas 10 µM ivermectin treatment killed 100% of adult lice after 24h, we obtained the same result with 10 µM lotilaner in only 3 hours following exposure. This fast activity is in accordance with the 4h-12h needed to kill ticks and fleas in lotilaner treated dogs [81,82]. Based on dog data, we can speculate that a single oral dose could provide a pediculicidal activity above 17 days corresponding to the complete life cycle of the human lice [9,19]. Therefore, the long-lasting activity of isoxazolines could overcome the absence of activity on embryonated eggs and also prevent re-infestations with a single oral dose. Considering its relatively benign toxicological profile for mammals along with rapid knockdown of lice, isoxazolines seems to be an excellent candidate drug to tackle louse infestations in humans. Nevertheless, the innocuity of isoxazolines towards human remains to be proven as well as its pharmacokinetics. Interestingly, Miglianico *et al.* recently reported the high efficacy of two other veterinarian drugs from the isoxazoline family (i.e afoxolaner and fluralaner) against a panel of insect species representing major vectors for human tropical diseases [83]. Computational modelling highlighted both the feasibility and the relevancy of using isoxazoline for human medication. In accordance, our results strongly support isoxazoline compounds as major candidates for drug repurposing alone or in co-administration with ivermectin. Indeed, new combinations of active compounds have become frequent in veterinary medicine (e.g. anthelmintics). Alike ivermectin, a useful feature of lotilaner is its mode of administration through oral route, which is more tractable to human than topical formulations. Since ivermectin and lotilaner are efficient at killing human lice, it is tempting to suggest that a combination of both drugs may have a considerable potential, resulting in an additive or a synergistic effect allowing the control of emerging ivermectin resistant lice and delay or overcome resistance. Such a therapeutic option was recently achieved with the release of fluralaner combined with moxidectin [84,85], afoxolaner plus milbemycin oxime [86] and sarolaner combined either with selamectin [87,88] or moxidectin and pyrantel on the veterinary market for small animals [89]. Hence, it is reasonable to conclude that further investigations on the efficacy of lotilaner alone or in combination with ivermectin for general use as pediculicides would be particularly pertinent and justified. We hope that the results presented here contribute to an increased understanding on the mechanisms behind the physiology of neurotransmission and of the mode of action of the pediculicidal drugs in body lice at the functional level and will provide new therapeutic strategies to ensure the sustainable and effective control of louse infestations.

Methods

Ethics statement

All animal care and experimental procedures were conducted in strict accordance with the European guidelines for the care and use of laboratory animals and were approved by French

Ministry for Research and the regional Val de Loire ethics committee (no 19) as a protocol registered under the permit number APAFIS#8455–2017010616224913 v3.

Chemical assays on body lice

The colony of human body lice (*Pediculus humanus humanus*) were provided by Kosta Y. Mumcuoglu from the Kuvin Center for the Study of Infectious and Tropical Diseases, Hebrew University-Hadassah Medical School, Jerusalem, Israel. This laboratory-reared colony adapted to rabbit blood were fed four times per week for 20–30 min on rabbits and maintained at 30 ± 1˚C and 60–70% relative humidity without exposure to any drugs [90]. Survival and immobilization were monitored by microscopical observations at 1, 2, 3 and 24 h after contact of 44 lice at different stages of the life cycle with insecticides at concentrations ranging from 1 to 100 μM or 1% DMSO on a Whatman grade 1 filter paper in a 55 mm Petri dish following the knockdown classification from KD$^+$ to KD^{++++} (S1 Table), as previously described [12]. Nits (50 to 190 per condition) were incubated with lotilaner or ivermectin and hatching was monitored between six and nine days. Water and solution of 1% DMSO were used as negative controls. Pictures were recorded with a Motic Digital Microscope 143 Series and the Motic Image Plus 3.0 software.

Cloning of full-length cDNA sequences of *GluCl* and *rdl* from *Pediculus humanus humanus*

Total RNA was extracted from 30 mg of lice (15 lice) using the Total RNA isolation Nucleospin RNA kit (Macherey-Nagel) according to the manufacturer's recommendations. Complementary DNA (cDNA) was synthesized using the GeneRacer kit with the SuperScript III reverse transcriptase (Invitrogen) following the manufacturer's recommendations. Using the *A. mellifera* and *D. melanogaster* GluCl and RDL subunit sequences as querries, tBLASTn searches in NCBI (http://blast.ncbi.nlm.nih.gov/Blast.cgi) allowed the identification of partial genomic contigs (AAZO01006897 and AAZO01005501 for *Phh-glucl* and AAZO01005738, AAZO01000267 and AAZO01000266 for *Phh-rdl*) and partial mRNA sequences (XM_002429761 for *Phh-GluCl* and XM_002422861.1 for *Phh-rdl*) containing the 3' cDNA ends. Primers designed on the sequences retrieved from the BLAST searches are reported in **S3 Table**. Then, the corresponding 5' cDNA ends were obtained by RLM-RACE experiments using the Generacer kit with two rounds of PCR as described elsewhere [91]. After the identification of the cDNA 5' ends, new primers were designed. The full-length complete coding sequences of *Phh-GluCl* and *Phh-rdl* were subsequently amplified by nested PCRs with the proofreading Phusion High-Fidelity DNA Polymerase (Thermo Scientific) using two pairs of primers. Then, PCR products were cloned into the transcription vector pTB-207 [92] using the In-Fusion HD Cloning kit (Clontech) as described previously [93]. Recombinant plasmid DNA was purified using EZNA Plasmid DNA Mini kit (Omega Bio-Tek) and the sequences were checked (Eurofins Genomics). The novel complete coding sequences of the two Phh-GluCl and Phh-RDL subunits were deposited to Genbank under the accession numbers MT321070 to MT321073. The constructions were linearized with the MlsI restriction enzyme (Thermofisher) and cRNAs were synthetized *in vitro* using the mMessage mMachine T7 transcription kit following the manufacturer's recommendations (Ambion). Lithium chloride-precipitated cRNAs were resuspended in RNAse-free water and stored at -20˚C.

Sequence analysis and phylogeny

Signal peptide and transmembrane domain were predicted using SignalP4.1 [94] and SMART [95], respectively. Deduced amino-acid sequences of Phh-GluCl and Phh-RDL were aligned

using the MUSCLE algorithm [96] and further processed with GeneDoc (IUBio). The phylogenetic distance trees were generated on amino-acid sequences by the SeaView software [97] using BioNJ Poisson parameters and bootstrap values were calculated with 1000 replicates as described previously [98]. The resulting trees were modified by FigTree (http://tree.bio.ed.ac.uk/software/figtree/). The accession numbers for the protein sequences mentioned in this article are: *Apis mellifera* (Ame): GluCl ABG75737, GRD AJE68942, LCCH3 AJE68943, RDL AJE68941, CG8916 NP_001071290; nAChR7 AJE70265; *Ctenocephalides felis* (Cfe): RDL AHE41088; *Drosophila melanogaster* (Dme): GluCl AAC47266, GRD NP_524131, LCCH3 NP_996469, RDL NP_523991, CG8916 NP_001162770; *Ixodes scapularis* (Isc): GluCl ALF36853; *Musca domestica* (Mdo): GluCl BAD16657, RDL NP_001292048; *Pediculus humanus humanus* (Phh): GluCl1 MT321070, GluCl2 MT321071, RDL1 MT321072, RDL2 MT321073; *Rhipicephalus microplus* (Rmi): GluCl AHE41097, RDL AHE41094; *Tetranychus urticae* (Tur): GluCl BAJ41378 and *Tribolium castaneum* (Tca): GluCl NP_001107775, GRD NP_001107772, LCCH3 NP_001103251, RDL NP_001107809, 8916 NP_001103425.

Electrophysiology in *Xenopus laevis* oocytes and data analysis

Defolliculated *Xenopus laevis* oocytes were purchased from Ecocyte Bioscience and maintained in incubation solution (100 mM NaCl, 2 mM KCl, 1.8 mM $CaCl_2.2H_2O$, 1 mM $MgCl_2.6H_2O$, 5 mM HEPES, 2.5 mM $C_3H_3NaO_3$, pH 7.5 supplemented with penicillin 100 U/mL and streptomycin 100 μg/mL) at 19°C. Each oocyte was microinjected with 57 ng of cRNA encoding Phh-GluCl or Phh-RDL using a Drummond nanoject II microinjector. Three to five days after cRNA injection, two-electrode voltage-clamp recordings were performed with an oocyte clamp OC-725C amplifier (Warner instrument) at a holding potential of -80mV or -60 mV to assess the expression of the GluCl or RDL channels. Currents were recorded and analyzed using the pCLAMP 10.4 package (Molecular Devices). Concentration-response relationships for agonists were carried out by challenging oocytes with 10 s applications of increasing concentrations of compounds. The peak current values were normalized to the response to 1000 μM glutamate or 100 μM GABA giving the maximum current amplitude for GluCl and RDL channels, respectively. For Phh-GluCl, the dose-response relationship for ivermectin was performed by applying each concentration of ivermectin for 20–30 s. Each oocyte received only one ivermectin concentration ($\leq$ 30 nM) followed with a high ivermectin concentration ($\geq$ 100 nM). Data were normalized to a first 100 μM glutamate apllication. For RDL, the effect of antagonists was evaluated, by a first preincubation of each antagonist alone for 90 s, followed by the co-application with 100 μM GABA for 10 s. Oocytes were then washed with recording buffer and sequentially preincubated with an increasing antagonist concentration followed by coapplication with 100 μM GABA. The observed responses were normalized to the response induced by 100 μM GABA alone performed prior to challenging with the antagonist. The concentration of agonist required to mediate 50% of the maximum response (EC_{50}), the concentration of antagonist required to inhibit 50% of the agonist response (IC_{50}) and the Hill coefficient (nH) were determined using non-linear regression on normalized data with GraphPad Prism software. Concentration-response curves for agonists were fitted with the following equation:

$$Y = \frac{100}{1 + 10^{H(logEC50-X)}}$$

Where Y is the normalized response, H is the Hill slope and X is the logarithm of concentration. The same equation was used for the concentration-response curves for antagonists by replacing $logEC_{50}$ by $logIC_{50}$. Results are expressed as mean +/- SEM and statistical analysis

were performed using One-Way ANOVA with Tukey's Multiple Comparisons Test. The competitive experiments on Phh-RDL were performed as previously described [42] with a concentration-response relationship in the presence of GABA alone or with 1 nM or 10 nM lotilaner. A pre-incubation of 1 nM or 10 nM lotilaner for 90 s was followed by a coapplication with increasing concentrations of GABA (1–1000 μM) for 10 s with a 30 s wash between each concentration. Current amplitudes were normalized with a first 100 μM GABA application. The corresponding concentration response curves were fitted using the following four parameter Hill equation:

$$Y = \frac{\text{Bottom} + (\text{Top} - \text{Bottom})}{1 + 10^{H(LogEC50-X)}}$$

Where Bottom is the response at the minimal concentration and Top is the maximal response. Statistical comparison were performed using unpaired Student's t test. Chloride and sodium permeabilities were conducted as described previously [53]. In brief, the reversal potential of the GABA-induced currents was measured with a 1500-ms-long ramp of voltage from -60 to +60 mV in standard saline recording solution (100 mM NaCl, 2.5 mM KCl, 1 mM CaCl$_2$, 5 mM HEPES, pH 7.3) as well as in recording solutions containing a concentration range of either chloride (NaCl replaced by sodium acetate) or sodium (NaCl replaced by tetraethylammonium chloride).

Materials

Glutamate, GABA, fipronil, picrotoxin and ivermectin were purchased from Sigma-Aldrich. Glutamate and GABA were directly dissolved in recording solution. Fipronil, picrotoxin and ivermectin were first dissolved at 10–100 mM in DMSO and then diluted in recording solution to the final concentrations in which DMSO did not exceed 1%. Lotilaner (Credelio, Elanco, USA) was a commercial formulation purchased in a local pharmacy store. Tablets containing 450 mg lotilaner were dissolved in DMSO to obtain a 100 mM lotilaner stock solution and subsequently diluted in recording solution at a final DMSO concentration less than 0.003%.

Supporting information

S1 Fig. Comparison of insect and acari GluCl subunits. A. Alignment of GluCl subunit deduced amino-acid sequences from *Pediculus humanus humanus* (Phh), *Apis mellifera* (Ame), *Rhipicephalus microplus* (Rmi) and *Tribolium castaneum* (Tca). Predicted signal peptides in N-terminal are highlighted in grey. Amino acid differences between the GluCl-1 and GluCl-2 sequences of *P. humanus humanus* are highlighted in red. Amino acids conserved between all the sequences are highlighted in blue. The cys-loop, transmembrane domains (TM1-TM4) and the highly variable intracellular loop are indicated by the bars. **B.** Distance tree (BioNJ, Poisson) of GluCl protein sequences from insects and acari. The three letter prefixes in gene names Tur, Phh, Ame, Tca, Dme, Mdo, Rmi and Isc refer to the species *Tetranychus urticae*, *Pediculus humanus humanus*, *Apis mellifera*, *Tribolium castaneum*, *Drosophila melanogaster*, *Musca domestica*, *Rhipicephalus microplus* and *Ixodes scapularis*, respectively. The tree was rooted with the *A. mellifera* alpha7 nAChR subunit as an outgroup. Branch lengths are proportional to the number of substitutions per amino acid. Scale bar represents the number of substitutions per site. The bootstrap values are indicated next to each branch. Accession numbers for sequences used in the phylogenetic analysis are provided in the Methods section. The two GluCl sequences of interest are highlighted in blue.
(TIF)

S2 Fig. Comparison of insect and acari GABA subunits. A. Alignment of RDL subunit deduced amino-acid sequences from *Pediculus humanus humanus* (Phh), *Apis mellifera* (Ame), *Tribolium castaneum* (Tca) and *Rhipicephalus microplus* (Rmi). Predicted signal peptides in N-terminal are highlighted in grey. Amino acid difference between the RDL-1 and RDL-2 sequences of *P. humanus humanus* are highlighted in red. Amino acids conserved between all the sequences are highlighted in blue. The cys-loop, predicted transmembrane domains (TM1-TM4) and the highly variable intracellular loop are indicated by the bars. **B.** Distance tree (BioNJ, Poisson) of GABACl protein sequence from insects and acari. The three letter prefixes in gene names Phh, Ame, Cfe, Tca, Dme, Mdo and Rmi refer to the species *Pediculus humanus humanus*, *Apis mellifera*, *Ctenocephalides felis*, *Tribolium castaneum*, *Drosophila melanogaster*, *Musca domestica* and *Rhipicephalus microplus*, respectively. The tree was rooted with the *A. mellifera* alpha7 nAChR subunit as an outgroup. Branch lengths are proportional to the number of substitutions per amino acid. Scale bar represents the number of substitutions per site. The bootstrap values are indicated next to each branch. Accession numbers for sequences used in the phylogenetic analysis are provided in the Methods section. The two RDL sequences of interest are highlighted in purple.
(TIF)

S3 Fig. Current traces of uninjected oocytes and oocytes injected with Phh-GluCl-2 or Phh-RDL-2. A. Current traces of uninjected oocytes after application of glutamate and GABA at 100 μM. The bar indicates the application time of 10 s. **B.** For Phh-GluCl-2, oocytes were clamped at -80mV and response to 100 μM of glutamate was measured (n = 11). For Phh-RDL-2, oocytes were clamped at -60mV and response to 100 μM of GABA was measured (n = 12). The bar indicates the application time of 10 s.
(TIF)

S4 Fig. Agonistic effect of ivermectin on GABA-elicited currents in *X. laevis* oocytes expressing Phh-RDL receptor. A. Representative current traces evoked by 100 μM GABA followed by 90 s application of 100 nM or 1 μM ivermectin. Application times are indicated by the bars. **B.** Concentration response curve of the ivermectin agonist effect. Data are normalized to a first 100 μM GABA application (mean +/- SEM, n = 5–13).
(TIF)

S1 Table. Knockdown groups. Lice from groups KD[+++] and KD[++++] were considered as dead [12].
(TIF)

S2 Table. Rates of mortality of *P. humanus humanus* exposed to lotilaner, ivermectin, fipronil and picrotoxin.
(TIF)

S3 Table. Primers used for the PCR and cloning of *P. humanus humanus* GluCl and RDL subunits.
(TIF)

Acknowledgments

Author Contributions

Conceptualization: Nicolas Lamassiaude, Berthine Toubate, Cédric Neveu, Françoise Debierre-Grockiego, Isabelle Dimier-Poisson, Claude L. Charvet.

Formal analysis: Nicolas Lamassiaude, Berthine Toubate, Pierre Charnet, Françoise Debierre-Grockiego, Claude L. Charvet.

Funding acquisition: Berthine Toubate, Cédric Neveu, Isabelle Dimier-Poisson.

Investigation: Nicolas Lamassiaude, Berthine Toubate, Pierre Charnet, Catherine Dupuy, Claude L. Charvet.

Methodology: Nicolas Lamassiaude, Berthine Toubate, Cédric Neveu, Françoise Debierre-Grockiego, Isabelle Dimier-Poisson, Claude L. Charvet.

Project administration: Isabelle Dimier-Poisson, Claude L. Charvet.

Resources: Berthine Toubate, Cédric Neveu, Isabelle Dimier-Poisson, Claude L. Charvet.

Supervision: Isabelle Dimier-Poisson, Claude L. Charvet.

Validation: Nicolas Lamassiaude, Berthine Toubate, Cédric Neveu, Pierre Charnet, Françoise Debierre-Grockiego, Isabelle Dimier-Poisson, Claude L. Charvet.

Visualization: Nicolas Lamassiaude, Berthine Toubate, Françoise Debierre-Grockiego.

Writing – original draft: Nicolas Lamassiaude, Berthine Toubate, Claude L. Charvet.

Writing – review & editing: Nicolas Lamassiaude, Berthine Toubate, Cédric Neveu, Françoise Debierre-Grockiego, Isabelle Dimier-Poisson, Claude L. Charvet.

References

1. Boutellis A, Abi-Rached L, Raoult D. The origin and distribution of human lice in the world. Infect Genet Evol. 2014; 23:209–17. https://doi.org/10.1016/j.meegid.2014.01.017 PMID: 24524985.

2. Falagas ME, Matthaiou DK, Rafailidis PI, Panos G, Pappas G. Worldwide prevalence of head lice. Emerg Infect Dis. 2008; 14(9):1493–4. https://doi.org/10.3201/eid1409.080368 PMID: 18760032; PubMed Central PMCID: PMC2603110.

3. Al-Shahrani SA, Alajmi RA, Ayaad TH, Al-Shahrani MA, Shaurub EH. Genetic diversity of the human head lice, Pediculus humanus capitis, among primary school girls in Saudi Arabia, with reference to their prevalence. Parasitol Res. 2017; 116(10):2637–43. https://doi.org/10.1007/s00436-017-5570-3 PMID: 28803388.

4. Badiaga S, Brouqui P. Human louse-transmitted infectious diseases. Clin Microbiol Infect. 2012; 18 (4):332–7. https://doi.org/10.1111/j.1469-0691.2012.03778.x PMID: 22360386.

5. Liao CW, Cheng PC, Chuang TW, Chiu KC, Chiang IC, Kuo JH, et al. Prevalence of Pediculus capitis in schoolchildren in Battambang, Cambodia. J Microbiol Immunol Infect. 2019; 52(4):585–91. https://doi.org/10.1016/j.jmii.2017.09.003 PMID: 29150362.

6. Louni M, Mana N, Bitam I, Dahmani M, Parola P, Fenollar F, et al. Body lice of homeless people reveal the presence of several emerging bacterial pathogens in northern Algeria. PLoS Negl Trop Dis. 2018; 12(4):e0006397. https://doi.org/10.1371/journal.pntd.0006397 PMID: 29664950; PubMed Central PMCID: PMC5922582.

7. Ly TDA, Toure Y, Calloix C, Badiaga S, Raoult D, Tissot-Dupont H, et al. Changing Demographics and Prevalence of Body Lice among Homeless Persons, Marseille, France. Emerg Infect Dis. 2017; 23 (11):1894–7. https://doi.org/10.3201/eid2311.170516 PMID: 29048280; PubMed Central PMCID: PMC5652409.

8. Nejati J, Keyhani A, Tavakoli Kareshk A, Mahmoudvand H, Saghafipour A, Khoraminasab M, et al. Prevalence and Risk Factors of Pediculosis in Primary School Children in South West of Iran. Iran J Public Health. 2018; 47(12):1923–9. PMID: 30788308; PubMed Central PMCID: PMC6379608.

9. Veracx A, Raoult D. Biology and genetics of human head and body lice. Trends Parasitol. 2012; 28 (12):563–71. https://doi.org/10.1016/j.pt.2012.09.003 PMID: 23069652.

10. Kirkness EF, Haas BJ, Sun W, Braig HR, Perotti MA, Clark JM, et al. Genome sequences of the human body louse and its primary endosymbiont provide insights into the permanent parasitic lifestyle. Proc Natl Acad Sci U S A. 2010; 107(27):12168–73. https://doi.org/10.1073/pnas.1003379107 PMID: 20566863; PubMed Central PMCID: PMC2901460.

11. Olds BP, Coates BS, Steele LD, Sun W, Agunbiade TA, Yoon KS, et al. Comparison of the transcriptional profiles of head and body lice. Insect Mol Biol. 2012; 21(2):257–68. https://doi.org/10.1111/j.1365-2583.2012.01132.x PMID: 22404397.

12. Combescot-Lang C, Vander Stichele RH, Toubate B, Veirron E, Mumcuoglu KY. Ex vivo effectiveness of French over-the-counter products against head lice (Pediculus humanus capitis De Geer, 1778). Parasitol Res. 2015; 114(5):1779–92. https://doi.org/10.1007/s00436-015-4363-9 PMID: 25716822.

13. Izri A, Uzzan B, Maigret M, Gordon MS, Bouges-Michel C. Clinical efficacy and safety in head lice infection by Pediculus humanis capitis De Geer (Anoplura: Pediculidae) of a capillary spray containing a silicon-oil complex. Parasite. 2010; 17(4):329–35. https://doi.org/10.1051/parasite/2010174329 PMID: 21275239.

14. Diamantis SA, Morrell DS, Burkhart CN. Treatment of head lice. Dermatol Ther. 2009; 22(4):273–8. https://doi.org/10.1111/j.1529-8019.2009.01242.x PMID: 19580574.

15. Frankowski BL. American Academy of Pediatrics guidelines for the prevention and treatment of head lice infestation. Am J Manag Care. 2004; 10(9 Suppl):S269–72. PMID: 15515631

16. Clark JM, Yoon KS, Lee SH, Pittendrigh BR. Human lice: Past, present and future control. Pestic Biochem Phys. 2013; 106(3):162–71. https://doi.org/10.1016/j.pestbp.2013.03.008 WOS:000321805100013.

17. Downs AM, Stafford KA, Harvey I, Coles GC. Evidence for double resistance to permethrin and malathion in head lice. Br J Dermatol. 1999; 141(3):508–11. https://doi.org/10.1046/j.1365-2133.1999.03046.x PMID: 10583056.

18. Durand R, Bouvresse S, Berdjane Z, Izri A, Chosidow O, Clark JM. Insecticide resistance in head lice: clinical, parasitological and genetic aspects. Clin Microbiol Infect. 2012; 18(4):338–44. https://doi.org/10.1111/j.1469-0691.2012.03806.x PMID: 22429458.

19. Lebwohl M, Clark L, Levitt J. Therapy for head lice based on life cycle, resistance, and safety considerations. Pediatrics. 2007; 119(5):965–74. https://doi.org/10.1542/peds.2006-3087 PMID: 17473098.

20. Idriss S, Levitt J. Malathion for head lice and scabies: treatment and safety considerations. J Drugs Dermatol. 2009; 8(8):715–20. PMID: 19663108.

21. Eisenhower C, Farrington EA. Advancements in the treatment of head lice in pediatrics. J Pediatr Health Care. 2012; 26(6):451–61; quiz 62–4. https://doi.org/10.1016/j.pedhc.2012.05.004 PMID: 23099312.

22. Nolan K, Kamrath J, Levitt J. Lindane toxicity: a comprehensive review of the medical literature. Pediatr Dermatol. 2012; 29(2):141–6. https://doi.org/10.1111/j.1525-1470.2011.01519.x PMID: 21995612.

23. Guyton KZ, Loomis D, Grosse Y, El Ghissassi F, Benbrahim-Tallaa L, Guha N, et al. Carcinogenicity of tetrachlorvinphos, parathion, malathion, diazinon, and glyphosate. Lancet Oncol. 2015; 16(5):490–1. https://doi.org/10.1016/S1470-2045(15)70134-8 PMID: 25801782.

24. Richardson JR, Taylor MM, Shalat SL, Guillot TS 3rd, Caudle WM, Hossain MM, et al. Developmental pesticide exposure reproduces features of attention deficit hyperactivity disorder. FASEB J. 2015; 29 (5):1960–72. https://doi.org/10.1096/fj.14-260901 PMID: 25630971; PubMed Central PMCID: PMC4415012.

25. Humans IWGotEoCRt. Some Organophosphate Insecticides and Herbicides. Some Organophosphate Insecticides and Herbicides. IARC Monographs on the Evaluation of Carcinogenic Risks to Humans. Lyon (FR)2017. PMID: 31829533

26. Laing R, Gillan V, Devaney E. Ivermectin—Old Drug, New Tricks? Trends Parasitol. 2017; 33(6):463–72. https://doi.org/10.1016/j.pt.2017.02.004 PMID: 28285851; PubMed Central PMCID: PMC5446326.

27. Strycharz JP, Yoon KS, Clark JM. A new ivermectin formulation topically kills permethrin-resistant human head lice (Anoplura: Pediculidae). J Med Entomol. 2008; 45(1):75–81. https://doi.org/10.1603/0022-2585(2008)45[75:aniftk]2.0.co;2 PMID: 18283945.

28. Sanchezruiz WL, Nuzum DS, Kouzi SA. Oral ivermectin for the treatment of head lice infestation. Am J Health Syst Pharm. 2018; 75(13):937–43. https://doi.org/10.2146/ajhp170464 PMID: 29789316.

29. Amanzougaghene N, Fenollar F, Raoult D, Mediannikov O. Where Are We With Human Lice? A Review of the Current State of Knowledge. Front Cell Infect Microbiol. 2019; 9:474. https://doi.org/10.3389/fcimb.2019.00474 PMID: 32039050; PubMed Central PMCID: PMC6990135.

30. Amanzougaghene N, Fenollar F, Diatta G, Sokhna C, Raoult D, Mediannikov O. https://doi.org/10.1016/j.ijantimicag.2018.07.005 PMID: 30055248. Int J Antimicrob Agents. 2018; 52(5):593–8.

31. Amanzougaghene N, Fenollar F, Nappez C, Ben-Amara A, Decloquement P, Azza S, et al. Complexin in ivermectin resistance in body lice. PLoS Genet. 2018; 14(8):e1007569. https://doi.org/10.1371/journal.pgen.1007569 PMID: 30080859; PubMed Central PMCID: PMC6108520.

32. Ffrench-Constant RH, Williamson MS, Davies TG, Bass C. Ion channels as insecticide targets. J Neurogenet. 2016; 30(3–4):163–77. https://doi.org/10.1080/01677063.2016.1229781 PMID: 27802784; PubMed Central PMCID: PMC6021766.

33. Wolstenholme AJ. Glutamate-gated chloride channels. J Biol Chem. 2012; 287(48):40232–8. https://doi.org/10.1074/jbc.R112.406280 PMID: 23038250; PubMed Central PMCID: PMC3504739.

34. Claxton DP, Gouaux E. Expression and purification of a functional heteromeric GABAA receptor for structural studies. PLoS One. 2018; 13(7):e0201210. https://doi.org/10.1371/journal.pone.0201210 PMID: 30028870; PubMed Central PMCID: PMC6054424.

35. Cully DF, Paress PS, Liu KK, Schaeffer JM, Arena JP. Identification of a Drosophila melanogaster glutamate-gated chloride channel sensitive to the antiparasitic agent avermectin. J Biol Chem. 1996; 271 (33):20187–91. https://doi.org/10.1074/jbc.271.33.20187 PMID: 8702744.

36. ffrench-Constant RH, Steichen JC, Rocheleau TA, Aronstein K, Roush RT. A single-amino acid substitution in a gamma-aminobutyric acid subtype A receptor locus is associated with cyclodiene insecticide resistance in Drosophila populations. Proc Natl Acad Sci U S A. 1993; 90(5):1957–61. https://doi.org/10.1073/pnas.90.5.1957 PMID: 8095336; PubMed Central PMCID: PMC45999.

37. Ffrench-Constant RH, Rocheleau TA, Steichen JC, Chalmers AE. A point mutation in a Drosophila GABA receptor confers insecticide resistance. Nature. 1993; 363(6428):449–51. https://doi.org/10.1038/363449a0 PMID: 8389005.

38. Casida JE, Durkin KA. Novel GABA receptor pesticide targets. Pestic Biochem Physiol. 2015; 121:22–30. https://doi.org/10.1016/j.pestbp.2014.11.006 PMID: 26047108.

39. Gassel M, Wolf C, Noack S, Williams H, Ilg T. The novel isoxazoline ectoparasiticide fluralaner: Selective inhibition of arthropod gamma-aminobutyric acid- and L-glutamate-gated chloride channels and insecticidal/acaricidal activity. Insect Biochem Molec. 2014; 45:111–24. https://doi.org/10.1016/j.ibmb.2013.11.009 WOS:000331856900011. PMID: 24365472

40. Shoop WL, Hartline EJ, Gould BR, Waddell ME, McDowell RG, Kinney JB, et al. Discovery and mode of action of afoxolaner, a new isoxazoline parasiticide for dogs. Vet Parasitol. 2014; 201(3–4):179–89. https://doi.org/10.1016/j.vetpar.2014.02.020 PMID: 24631502.

41. McTier TL, Chubb N, Curtis MP, Hedges L, Inskeep GA, Knauer CS, et al. Discovery of sarolaner: A novel, orally administered, broad-spectrum, isoxazoline ectoparasiticide for dogs. Vet Parasitol. 2016; 222:3–11. https://doi.org/10.1016/j.vetpar.2016.02.019 PMID: 26961590.

42. Rufener L, Danelli V, Bertrand D, Sager H. The novel isoxazoline ectoparasiticide lotilaner (Credelio (TM)): a non-competitive antagonist specific to invertebrates gamma-aminobutyric acid-gated chloride channels (GABACIs). Parasite Vector. 2017; 10. ARTN 530 https://doi.org/10.1186/s13071-017-2470-4 WOS:000414159300005. PMID: 29089046

43. Ozoe Y, Asahi M, Ozoe F, Nakahira K, Mita T. The antiparasitic isoxazoline A1443 is a potent blocker of insect ligand-gated chloride channels. Biochem Bioph Res Co. 2010; 391(1):744–9. https://doi.org/10.1016/j.bbrc.2009.11.131 WOS:000273624500130. PMID: 19944072

44. Weber T, Selzer PM. Isoxazolines: A Novel Chemotype Highly Effective on Ectoparasites. ChemMedChem. 2016; 11(3):270–6. Epub 2016/01/07. https://doi.org/10.1002/cmdc.201500516 PMID: 26733048.

45. Selzer PM, Epe C. Antiparasitics in Animal Health: Quo Vadis? Trends Parasitol. 2020. Epub 2020/10/12. https://doi.org/10.1016/j.pt.2020.09.004 PMID: 33039282.

46. Sheng CW, Jia ZQ, Liu D, Wu HZ, Luo XM, Song PP, et al. Insecticidal spectrum of fluralaner to agricultural and sanitary pests. J Asia-Pac Entomol. 2017; 20(4):1213–8. https://doi.org/10.1016/j.aspen.2017.08.021 WOS:000419749300023.

47. Downs AMR, Stafford KA, Coles GC. Susceptibility of British head lice, Pediculus capitis, to imidacloprid and fipronil. Med Vet Entomol. 2000; 14(1):105–7. https://doi.org/10.1046/j.1365-2915.2000.00216.x WOS:000086260100017. PMID: 10759321

48. Keramidas A, Moorhouse AJ, Peter PR, Barry PH. Ligand-gated ion channels: mechanisms underlying ion selectivity. Prog Biophys Mol Bio. 2004; 86(2):161–204. https://doi.org/10.1016/j.pbiomolbio.2003.09.002 WOS:000223500100001. PMID: 15288758

49. Marais E, Klok CJ, Terblanche JS, Chown SL. Insect gas exchange patterns: a phylogenetic perspective. J Exp Biol. 2005; 208(23):4495–507. https://doi.org/10.1242/jeb.01928 WOS:000234414800023. PMID: 16339869

50. Eguchi Y, Ihara M, Ochi E, Shibata Y, Matsuda K, Fushiki S, et al. Functional characterization of Musca glutamate- and GABA-gated chloride channels expressed independently and coexpressed in Xenopus

oocytes. Insect Mol Biol. 2006; 15(6):773–83. https://doi.org/10.1111/j.1365-2583.2006.00680.x PMID: 17201770.

51. Cornejo I, Andrini O, Niemeyer MI, Maraboli V, Gonzalez-Nilo FD, Teulon J, et al. Identification and functional expression of a glutamate- and avermectin-gated chloride channel from Caligus rogercres-seyi, a southern Hemisphere sea louse affecting farmed fish. PLoS Pathog. 2014; 10(9):e1004402. https://doi.org/10.1371/journal.ppat.1004402 PMID: 25255455; PubMed Central PMCID: PMC4177951.

52. Furutani S, Ihara M, Lees K, Buckingham SD, Partridge FA, David JA, et al. The fungal alkaloid Okara-mine-B activates an L-glutamate-gated chloride channel from Ixodes scapularis, a tick vector of Lyme disease. Int J Parasitol Drugs Drug Resist. 2018; 8(2):350–60. https://doi.org/10.1016/j.ijpddr.2018.06.001 PMID: 29957333; PubMed Central PMCID: PMC6039357.

53. Menard C, Folacci M, Brunello L, Charreton M, Collet C, Mary R, et al. Multiple combinations of RDL subunits diversify the repertoire of GABA receptors in the honey bee parasite Varroa destructor. J Biol Chem. 2018; 293(49):19012–24. https://doi.org/10.1074/jbc.RA118.005365 PMID: 30333227; PubMed Central PMCID: PMC6295728.

54. Chen R, Belelli D, Lambert JJ, Peters JA, Reyes A, Lan NC. Cloning and functional expression of a Dro-sophila gamma-aminobutyric acid receptor. Proc Natl Acad Sci U S A. 1994; 91(13):6069–73. https://doi.org/10.1073/pnas.91.13.6069 PMID: 8016117; PubMed Central PMCID: PMC44139.

55. Fuse T, Kita T, Nakata Y, Ozoe F, Ozoe Y. Electrophysiological characterization of ivermectin triple actions on Musca chloride channels gated by L-glutamic acid and gamma-aminobutyric acid. Insect Bio-chem Molec. 2016; 77:78–86. https://doi.org/10.1016/j.ibmb.2016.08.005 WOS:000385321700008. PMID: 27543424

56. Yang Y, Lv J, Gui B, Yin H, Wu X, Zhang Y, et al. A-to-I RNA editing alters less-conserved residues of highly conserved coding regions: implications for dual functions in evolution. RNA. 2008; 14(8):1516–25. https://doi.org/10.1261/rna.1063708 PMID: 18567816; PubMed Central PMCID: PMC2491475.

57. Buckingham SD, Biggin PC, Sattelle BM, Brown LA, Sattelle DB. Insect GABA receptors: Splicing, edit-ing, and targeting by antiparasitics and insecticides. Mol Pharmacol. 2005; 68(4):942–51. https://doi.org/10.1124/mol.105.015313 WOS:000232002500003. PMID: 16027231

58. Jones AK, Sattelle DB. The cys-loop ligand-gated ion channel gene superfamily of the red flour beetle, Tribolium castaneum. BMC Genomics. 2007; 8:327. https://doi.org/10.1186/1471-2164-8-327 PMID: 17880682; PubMed Central PMCID: PMC2064938.

59. Jones AK, Buckingham SD, Papadaki M, Yokota M, Sattelle BM, Matsuda K, et al. Splice-variant- and stage-specific RNA editing of the Drosophila GABA receptor modulates agonist potency. J Neurosci. 2009; 29(13):4287–92. https://doi.org/10.1523/JNEUROSCI.5251-08.2009 PMID: 19339622; PubMed Central PMCID: PMC6665385.

60. Taylor-Wells J, Senan A, Bermudez I, Jones AK. Species specific RNA A-to-I editing of mosquito RDL modulates GABA potency and influences agonistic, potentiating and antagonistic actions of ivermectin. Insect Biochem Mol Biol. 2018; 93:1–11. https://doi.org/10.1016/j.ibmb.2017.12.001 PMID: 29223796.

61. Liu F, Shi XZ, Liang YP, Wu QJ, Xu BY, Xie W, et al. A 36-bp deletion in the alpha subunit of glutamate-gated chloride channel contributes to abamectin resistance in Plutella xylostella. Entomol Exp Appl. 2014; 153(2):85–92. https://doi.org/10.1111/eea.12232 WOS:000344386700001.

62. Mermans C, Dermauw W, Geibel S, Van Leeuwen T. A G326E substitution in the glutamate-gated chlo-ride channel 3 (GluCl3) of the two-spotted spider mite Tetranychus urticae abolishes the agonistic activ-ity of macrocyclic lactones. Pest Management Science. 2017; 73(12):2413–8. https://doi.org/10.1002/ps.4677 WOS:000414177900003. PMID: 28736919

63. Wu SF, Mu XC, Dong YX, Wang LX, Wei Q, Gao CF. Expression pattern and pharmacological charac-terisation of two novel alternative splice variants of the glutamate-gated chloride channel in the small brown planthopper Laodelphax striatellus. Pest Manag Sci. 2017; 73(3):590–7. https://doi.org/10.1002/ps.4340 PMID: 27302648.

64. Xu ZF, Wu Q, Xu Q, He L. Functional Analysis Reveals Glutamate and Gamma-Aminobutyric Acid-Gated Chloride Channels as Targets of Avermectins in the Carmine Spider Mite. Toxicol Sci. 2017; 155 (1):258–69. https://doi.org/10.1093/toxsci/kfw210 WOS:000397041300022. PMID: 27742867

65. Atif M, Lynch JW, Keramidas A. The effects of insecticides on two splice variants of the glutamate-gated chloride channel receptor of the major malaria vector, Anopheles gambiae. Br J Pharmacol. 2020; 177(1):175–87. https://doi.org/10.1111/bph.14855 PMID: 31479507; PubMed Central PMCID: PMC6976876.

66. Garrood WT, Zimmer CT, Gutbrod O, Luke B, Williamson MS, Bass C, et al. Influence of the RDL A301S mutation in the brown planthopper Nilaparvata lugens on the activity of phenylpyrazole insecti-cides. Pestic Biochem Physiol. 2017; 142:1–8. https://doi.org/10.1016/j.pestbp.2017.01.007 PMID: 29107231; PubMed Central PMCID: PMC5672059.

67. ffrench-Constant RH, Rocheleau TA. Drosophila gamma-aminobutyric acid receptor gene Rdl shows extensive alternative splicing. J Neurochem. 1993; 60(6):2323–6. https://doi.org/10.1111/j.1471-4159.1993.tb03523.x PMID: 7684073.

68. Taylor-Wells J, Hawkins J, Colombo C, Bermudez I, Jones AK. Cloning and functional expression of intracellular loop variants of the honey bee (Apis mellifera) RDL GABA receptor. Neurotoxicology. 2017; 60:207–13. https://doi.org/10.1016/j.neuro.2016.06.007 WOS:000403133600025. PMID: 27288983

69. Jiang J, Huang LX, Chen F, Sheng CW, Huang QT, Han ZJ, et al. Novel alternative splicing of GABA receptor RDL exon 9 from Laodelphax striatellus modulates agonist potency. Insect Sci. 2020. https://doi.org/10.1111/1744-7917.12789 PMID: 32293803.

70. Lindley D. Merck's new drug free to WHO for river blindness programme. Nature. 1987; 329(6142):752. https://doi.org/10.1038/329752a0 PMID: 3670379.

71. Chosidow O, Giraudeau B, Cottrell J, Izri A, Hofmann R, Mann SG, et al. Oral ivermectin versus malathion lotion for difficult-to-treat head lice. N Engl J Med. 2010; 362(10):896–905. https://doi.org/10.1056/NEJMoa0905471 PMID: 20220184.

72. Ahmad HM, Abdel-Azim ES, Abdel-Aziz RT. Assessment of topical versus oral ivermectin as a treatment for head lice. Dermatol Ther. 2014; 27(5):307–10. https://doi.org/10.1111/dth.12144 PMID: 25041547.

73. Leulmi H, Diatta G, Sokhna C, Rolain JM, Raoult D. Assessment of oral ivermectin versus shampoo in the treatment of pediculosis (head lice infestation) in rural areas of Sine-Saloum, Senegal. Int J Antimicrob Agents. 2016; 48(6):627–32. https://doi.org/10.1016/j.ijantimicag.2016.07.014 PMID: 27866866.

74. Yoon KS, Strycharz JP, Baek JH, Sun W, Kim JH, Kang JS, et al. Brief exposures of human body lice to sublethal amounts of ivermectin over-transcribes detoxification genes involved in tolerance. Insect Mol Biol. 2011; 20(6):687–99. https://doi.org/10.1111/j.1365-2583.2011.01097.x PMID: 21895817; PubMed Central PMCID: PMC3208734.

75. Wei PL, Che WA, Wang JD, Xiao D, Wang R, Luo C. RNA interference of glutamate-gated chloride channel decreases abamectin susceptibility in Bemisia tabaci. Pestic Biochem Phys. 2018; 145:1–7. https://doi.org/10.1016/j.pestbp.2017.12.004 WOS:000428601100001. PMID: 29482724

76. Kane NS, Hirschberg B, Qian S, Hunt D, Thomas B, Brochu R, et al. Drug-resistant Drosophila indicate glutamate-gated chloride channels are targets for the antiparasitics nodulisporic acid and ivermectin. P Natl Acad Sci USA. 2000; 97(25):13949–54. https://doi.org/10.1073/pnas.240464697 WOS:000165728800088. PMID: 11095718

77. Wang XL, Puinean AM, O'Reilly AO, Williamson MS, Smelt CLC, Millar NS, et al. Mutations on M3 helix of Plutella xylostella glutamate-gated chloride channel confer unequal resistance to abamectin by two different mechanisms. Insect Biochem Molec. 2017; 86:50–7. https://doi.org/10.1016/j.ibmb.2017.05.006 WOS:000405055100006. PMID: 28576654

78. Nakata Y, Fuse T, Yamato K, Asahi M, Nakahira K, Ozoe F, et al. A Single Amino Acid Substitution in the Third Transmembrane Region Has Opposite Impacts on the Selectivity of the Parasiticides Fluralaner and Ivermectin for Ligand-Gated Chloride Channels. Mol Pharmacol. 2017; 92(5):546–55. https://doi.org/10.1124/mol.117.109413 WOS:000412893200006. PMID: 28887352

79. Yamato K, Nakata Y, Takashima M, Ozoe F, Asahi M, Kobayashi M, et al. Effects of intersubunit amino acid substitutions on GABA receptor sensitivity to the ectoparasiticide fluralaner. Pestic Biochem Physiol. 2020; 163:123–9. https://doi.org/10.1016/j.pestbp.2019.11.001 PMID: 31973848

80. Little SE. Lotilaner—a novel systemic tick and flea control product for dogs. Parasit Vectors. 2017; 10(1):539. https://doi.org/10.1186/s13071-017-2471-3 PMID: 29089062; PubMed Central PMCID: PMC5664799.

81. Cavalleri D, Murphy M, Seewald W, Drake J, Nanchen S. A randomised, blinded, controlled field study to assess the efficacy and safety of lotilaner tablets (Credelio) in controlling fleas in client-owned dogs in European countries. Parasit Vectors. 2017; 10(1):526. https://doi.org/10.1186/s13071-017-2479-8 PMID: 29089065; PubMed Central PMCID: PMC5664837.

82. Murphy M, Garcia R, Karadzovska D, Cavalleri D, Snyder D, Seewald W, et al. Laboratory evaluations of the immediate and sustained efficacy of lotilaner (Credelio) against four common species of ticks affecting dogs in North America. Parasit Vectors. 2017; 10(1):523. https://doi.org/10.1186/s13071-017-2476-y PMID: 29089057; PubMed Central PMCID: PMC5664823.

83. Miglianico M, Eldering M, Slater H, Ferguson N, Ambrose P, Lees RS, et al. Repurposing isoxazoline veterinary drugs for control of vector-borne human diseases. P Natl Acad Sci USA. 2018; 115(29):E6920–E6. https://doi.org/10.1073/pnas.1801338115 WOS:000438892600031. PMID: 29967151

84. Kohler-Aanesen H, Saari S, Armstrong R, Pere K, Taenzler J, Zschiesche E, et al. Efficacy of fluralaner (Bravecto chewable tablets) for the treatment of naturally acquired Linognathus setosus infestations on dogs. Parasit Vectors. 2017; 10(1):426. https://doi.org/10.1186/s13071-017-2344-9 PMID: 28923117; PubMed Central PMCID: PMC5604360.

85. Fisara P, Guerino F, Sun FS. Efficacy of a spot-on combination of fluralaner plus moxidectin (Bravecto ((R)) Plus) in cats following repeated experimental challenge with a field isolate of Ctenocephalides felis. Parasite Vector. 2019; 12. ARTN 259 https://doi.org/10.1186/s13071-019-3512-x WOS:000468877400001. PMID: 31122282

86. Beugnet F, Crafford D, de Vos C, Kok D, Larsen D, Fourie J. Evaluation of the efficacy of monthly oral administration of afoxolaner plus milbemycin oxime (NexGard Spectra((R)), Merial) in the prevention of adult Spirocerca lupi establishment in experimentally infected dogs. Vet Parasitol. 2016; 226:150–61. Epub 2016/08/16. https://doi.org/10.1016/j.vetpar.2016.07.002 PMID: 27514901.

87. Geurden T, Borowski S, Wozniakiewicz M, King V, Fourie J, Liebenberg J. Comparative efficacy of a new spot-on combination product containing selamectin and sarolaner (Stronghold (R) Plus) versus fluralaner (Bravecto (R)) against induced infestations with Ixodes ricinus ticks on cats. Parasite Vector. 2017; 10. ARTN 319 https://doi.org/10.1186/s13071-017-2259-5 WOS:000405900300003. PMID: 28662690

88. Vatta AF, King VL, Young DR, Chapin S. Efficacy of three consecutive monthly doses of a topical formulation of selamectin and sarolaner (Revolution((R)) Plus/Stronghold((R)) Plus) compared with a single dose of fluralaner (Bravecto((R)) for Cats) against induced infestations of Ctenocephalides felis on cats. Vet Parasitol. 2019; 270 Suppl 1:S52–S7. https://doi.org/10.1016/j.vetpar.2019.05.004 PMID: 31133494.

89. Becskei C, Fias D, Mahabir SP, Farkas R. Efficacy of a novel oral chewable tablet containing sarolaner, moxidectin and pyrantel (Simparica Trio) against natural flea and tick infestations on dogs presented as veterinary patients in Europe. Parasit Vectors. 2020; 13(1):72. Epub 2020/03/03. https://doi.org/10.1186/s13071-020-3946-1 PMID: 32113486; PubMed Central PMCID: PMC7049391.

90. Mumcuoglu KY, Danilevich M, Zelig O, Grinbaum H, Friger M, Meinking TL. Effects of blood type and blood handling on feeding success, longevity and egg production in the body louse, Pediculus humanus humanus. Med Vet Entomol. 2011; 25(1):12–6. https://doi.org/10.1111/j.1365-2915.2010.00897.x PMID: 20678099.

91. Courtot E, Charvet CL, Beech RN, Harmache A, Wolstenholme AJ, Holden-Dye L, et al. Functional Characterization of a Novel Class of Morantel-Sensitive Acetylcholine Receptors in Nematodes. PLoS Pathog. 2015; 11(12):e1005267. https://doi.org/10.1371/journal.ppat.1005267 PMID: 26625142; PubMed Central PMCID: PMC4666645.

92. Boulin T, Fauvin A, Charvet CL, Cortet J, Cabaret J, Bessereau JL, et al. Functional reconstitution of Haemonchus contortus acetylcholine receptors in Xenopus oocytes provides mechanistic insights into levamisole resistance. Br J Pharmacol. 2011; 164(5):1421–32. https://doi.org/10.1111/j.1476-5381.2011.01420.x PMID: 21486278; PubMed Central PMCID: PMC3221097.

93. Charvet CL, Guegnard F, Courtot E, Cortet J, Neveu C. Nicotine-sensitive acetylcholine receptors are relevant pharmacological targets for the control of multidrug resistant parasitic nematodes. Int J Parasitol Drugs Drug Resist. 2018; 8(3):540–9. https://doi.org/10.1016/j.ijpddr.2018.11.003 PMID: 30502120; PubMed Central PMCID: PMC6287576.

94. Petersen TN, Brunak S, von Heijne G, Nielsen H. SignalP 4.0: discriminating signal peptides from transmembrane regions. Nat Methods. 2011; 8(10):785–6. https://doi.org/10.1038/nmeth.1701 PMID: 21959131.

95. Schultz J, Milpetz F, Bork P, Ponting CP. SMART, a simple modular architecture research tool: identification of signaling domains. Proc Natl Acad Sci U S A. 1998; 95(11):5857–64. https://doi.org/10.1073/pnas.95.11.5857 PMID: 9600884; PubMed Central PMCID: PMC34487.

96. Edgar RC. MUSCLE: multiple sequence alignment with high accuracy and high throughput. Nucleic Acids Res. 2004; 32(5):1792–7. https://doi.org/10.1093/nar/gkh340 PMID: 15034147; PubMed Central PMCID: PMC390337.

97. Gouy M, Guindon S, Gascuel O. SeaView version 4: A multiplatform graphical user interface for sequence alignment and phylogenetic tree building. Mol Biol Evol. 2010; 27(2):221–4. https://doi.org/10.1093/molbev/msp259 PMID: 19854763.

98. Abongwa M, Buxton SK, Courtot E, Charvet CL, Neveu C, McCoy CJ, et al. Pharmacological profile of Ascaris suum ACR-16, a new homomeric nicotinic acetylcholine receptor widely distributed in Ascaris tissues. Br J Pharmacol. 2016; 173(16):2463–77. https://doi.org/10.1111/bph.13524 PMID: 27238203; PubMed Central PMCID: PMC4959957.